Tissue-restricted control of established central nervous system autoimmunity by TNF receptor 2–expressing Treg cells

Emilie Ronin, Charlotte Pouchy, Maryam Khosravi, Morgane Hilaire, Sylvie Grégoire, Armanda Casrouge, Sahar Kassem, David Sleurs, Gaëlle H Martin, Noémie Chanson, et al.

Tissue-restricted control of established central nervous system autoimmunity by TNF receptor 2-expressing Treg cells

Emilie Ronin[a,1], Charlotte Pouchy[a,1], Maryam Khosravi[a], Morgane Hilaire[a], Sylvie Grégoire[a], Armanda Casrouge[a], Sahar Kassem[a], David Sleurs[a], Gaëlle H Martin[a], Noémie Chanson[a], Yannis Lombardi[a], Guilhem Lalle[b], Harald Wajant[c], Cédric Auffray[d], Bruno Lucas[d], Gilles Marodon[a], Yenkel Grinberg-Bleyer[b,2,3] and Benoît L Salomon[a,2,3]

[a]Sorbonne Université, Inserm, CNRS, Centre d'Immunologie et des Maladies Infectieuses (CIMI)-Paris, 75013 Paris, France.

[b]Centre de Recherche en Cancérologie de Lyon, Labex DEVweCAN, Inserm, CNRS, Université Claude Bernard Lyon 1, Centre Léon Bérard, 69008 Lyon, France.

[c]Division Molecular Internal Medicine, Department of Internal Medicine II, University Hospital Würzburg, 97070, Würzburg, Germany.

[d]Institut Cochin, CNRS, Inserm, Paris Université, 75014 Paris, France

[1]E.R. and C.P. contributed equally to this work.

[2]Y.G.-B and B.L.S. contributed equally to this work.

[3]To whom correspondence may be addressed : Benoit Salomon, CIMI-Paris, 91 Bd de l'hopital, 75013 Paris, France, Tel: +33 140779769, benoit.salomon@inserm.fr. ORCID ID: 0000-0001-9673-5578. Yenkel Grinberg-Bleyer, CRCL, 28 rue Laennec, 69008 Lyon, France, Tel: +33 469856248, yenkel.grinberg-bleyer@inserm.fr. ORCID ID: 0000-0002-3515-8305.

Classification: Biological Sciences / Immunology and inflammation

Keywords: Treg cells, autoimmunity, EAE, tissue-restricted, TNF receptor 2, TNF, suppressive mechanism, CNS.

Author Contributions: YGB and BLS conceived the initial project; ER, CP, MK, MH, SG, AC, SK, DS, GHM, NC, YL, YGB and BLS performed experiments and analyzed data; ER, CP, YGB and BLS wrote the manuscript; GL, CA, BL, HW and GM provided some materials and critical discussions and reviewed the manuscript.

ABSTRACT

$CD4^+Foxp3^+$ regulatory T (Treg) cells are central modulators of autoimmune diseases. However, the timing and location of Treg cell-mediated suppression of tissue-specific autoimmunity remain undefined. Here, we addressed these questions by investigating the role of TNF receptor 2 (TNFR2) signaling in Treg cells during experimental autoimmune encephalomyelitis (EAE), a model of multiple sclerosis. We found that TNFR2 expressing Treg cells were critical to suppress EAE at peak disease in the central nervous system but had no impact on T cell priming in lymphoid tissues at disease onset. Mechanistically, TNFR2 signaling maintained functional Treg cells with sustained expression of CTLA-4 and Blimp1, allowing active suppression of pathogenic T cells in the inflamed central nervous system. This late effect of Treg cells was further confirmed by treating mice with TNF and TNFR2 agonists and antagonists. Our findings are the first to show that endogenous Treg cells specifically suppress an autoimmune disease by acting in the target tissue during overt inflammation. Moreover, they bring a mechanistic insight to some of the adverse effects of anti-TNF therapy in patients.

SIGNIFICANCE STATEMENT

Regulatory T (Treg) cells have been highlighted for their central function in limiting the severity of autoimmune diseases such as multiple sclerosis (MS). To date, the anatomical location and timing of this Treg cell-mediated suppression are unknown. In this report, in a mouse model of MS, we demonstrate that Treg cells inhibit the pathogenic process directly in the central nervous system during established disease, rather than in the pre-symptomatic phase. This protective function requires the surface expression of TNF receptor 2 by Treg cells, as its genetic ablation or antibody-mediated blockade worsens disease symptoms. Our data reveal a unique function of Treg cells in autoimmunity and highlight TNFR2 as a promising therapeutic target.

INTRODUCTION

$CD4^+Foxp3^+$ regulatory T (Treg) cells play a pivotal role in the control of immune responses. In particular, the effector Treg cell subset, controlled in part by the master transcription factor Blimp-1 (1-3), exerts a critical role in the protection against autoimmune diseases by inhibiting autoreactive cells. Perturbations in Treg cell numbers or function trigger or exacerbate autoimmune diseases in mice and humans, such as type 1 diabetes, rheumatoid arthritis or experimental autoimmune encephalomyelitis (EAE), a mouse model of multiple sclerosis (MS) (4, 5). In line with this latter observation, Treg cell depletion increased EAE symptoms (6), while transfer of polyclonal or myelin-reactive Treg cells limited the disease (7, 8). However, it is still unknown whether Treg cells suppress the priming of pathogenic conventional T (Tconv) cells in the draining lymph nodes (dLN) at disease onset, and/or inhibit their function directly in the central nervous system (CNS) in the phase of ongoing inflammation.

Our group and others have reported that TNF increased the proliferation of Treg cells via TNF receptor 2 (TNFR2) while maintaining or enhancing their suppressive function in vitro and in different immune-pathologies (9-13). This intriguing immune-regulatory facet of TNF is clearly exemplified in EAE. Mice deficient for TNFR2 exhibited aggravated symptoms of EAE, which was associated with lower Treg cell proportions in the CNS (14). In the same line, mice genetically engineered to express the human version of TNF, and in which TNFR2 was ablated in Treg cells, developed severe EAE symptoms (15). These studies suggested that the TNF/TNFR2 axis is central in Treg cell-mediated suppression of autoimmunity. However, the location and timing of this Treg cell-mediated suppression are currently unknown. Here, we addressed these questions by using constitutive and inducible ablation of TNFR2 in mature Treg cells. We showed that TNFR2

expressing Treg cells suppressed EAE locally in the inflamed CNS on established disease, without affecting pathogenic T cell priming in the dLN.

RESULTS

TNFR2 expression by hematopoietic cells is required to limit EAE severity and promotes Treg cell-intrinsic expansion in the CNS

Since TNFR2 is up-regulated in Treg cells upon activation (9), we analyzed its expression after EAE induction. The receptor was highly and preferentially expressed in Treg cells at all time points in dLN and from day 10 in the inflamed CNS (Fig. S1). To study the role of the TNF/TNFR2 axis in Treg cells during EAE, we first performed experiments with mice carrying germline deletion of TNFR2 (*Tnfrsf1b*$^{-/-}$, hereafter named 'KO'). As previously observed (16-18), KO mice exhibited normal CD4^{+} T cell numbers but had reduced Treg cell numbers in the spleen at steady state (Fig. S2). These mice developed more severe EAE than wild type (WT) controls, which was associated with reduced Treg cell accumulation in the inflamed CNS (Fig. S3*A and B*). We then generated bone marrow chimeric mice to assess the role of TNFR2 expression by hematopoietic and non-hematopoietic cells. Ablation of TNFR2 in the immune system, but not in the non-hematopoietic compartment, led to exacerbated EAE and reduced Treg cell numbers in the CNS (Fig. S3 *C-F*). This role of TNFR2 in Treg cell expansion was a cell-autonomous mechanism, as revealed by their reduced numbers in the competitive environment of mixed bone marrow chimeras (Fig. S3*G*).

TNFR2 signaling in Treg cells mediates disease suppression during overt CNS inflammation.

To further delineate the cell-autonomous role of TNFR2 in Treg cell biology, we generated mice with conditional ablation of TNFR2 in Treg cells by crossing mice expressing the CRE-recombinase in Treg cells (*Foxp3*^{Cre}) with mice carrying floxed *Tnfrsf1b* alleles (*Tnfrsf1b*^{fl}). It was critical to compare these *Foxp3*^{Cre}*Tnfrsf1b*^{fl} (hereafter named conditional knock-out or 'cKO') mice to their proper controls, the *Foxp3*^{Cre} mice, because of putative toxic effect of Cre expression, as recently reported (19, 20). As expected, Treg cells of cKO mice had complete ablation of TNFR2

expression (Fig. S4*A*). However, a partial decreased TNFR2 expression was also observed on Tconv cells, which was likely due to leakiness of Cre expression in non-Treg cells in *Foxp3*^{Cre} mice, previously reported in other mouse models (21, 22). cKO mice had no sign of spontaneous autoimmunity and displayed normal body weight (Fig. S4*B*). Treg cell proportion, numbers and expression of Foxp3, CD25 and CTLA-4 in lymphoid tissues were unaltered (Fig. S4 *C and D*). Also, the *in vitro* suppressive capacity of Treg cells was not or slightly reduced by TNFR2 ablation (Fig. S4 *E and F*). Therefore, TNFR2 is mainly dispensable for Treg cell homeostasis at steady state.

Next, we explored the cell-autonomous function of TNFR2 in Treg cells during CNS inflammation. Strikingly, compared to controls, cKO mice developed a very severe EAE leading to death in almost half of the mice by day 15 (Fig. 1A). This was not associated with increased total leukocytes infiltration in the CNS or dLN (Fig. S5*A*). Treg cell proportions were only transiently reduced at day 10 in the CNS of cKO mice (Fig. 1B, and Fig. S5*B*) and the overall level of Foxp3, Ki67, CD25 or Helios was unaltered (Fig. S5*D*). Also, TNFR2-deficient Treg cells did not acquire the capacity to produce pathogenic cytokines, such as IFNγ, IL-17A or GM-CSF after phorbol 12-myristate 13-acetate (PMA) ionomycin stimulation in the CNS (Fig. S5 *E and F*). However, further examination showed that these Treg cells in the CNS of cKO mice exhibited lower expression of CTLA-4, Blimp-1 and ICOS (Fig. 1 *C and D and* Fig. S5*C*), which are markers of effector Treg cells (1, 23, 24). Interestingly, these quantitative and phenotypic Treg cell alterations in the CNS were not observed in the spleen or dLN. To further investigate whether TNFR2^{+} Treg cell-mediated suppression of EAE occurs during the priming or effector phase, we used an inducible Cre system allowing TNFR2 ablation in Treg cells upon tamoxifen treatment. We thus generated *Foxp3*$^{Cre\text{-}ERT2}$*Tnfrsf1b*^{fl} (hereafter named induced conditional KO or 'icKO') mice. Importantly, in most of

these mice, tamoxifen administration induced TNFR2 ablation in Treg cells as efficiently as in cKO mice but not at all in Tconv cells (Fig. S6*A*). This icKO model is thus of great interest since TNFR2 ablation is Treg cell-specific contrary to cKO mice. To assess whether EAE control by TNFR2-expressing Treg cells is taking place in the CNS after disease onset, we administered tamoxifen from day 7 to 14 after disease induction. Remarkably, EAE severity was dramatically increased in icKO when compared to *Foxp3*$^{Cre\text{-}ERT2}$ control animals, similarly to what we observed with cKO mice (Fig. 2*A*). At day 14, total leukocyte numbers, Treg cell proportions and numbers as well as their Foxp3 expression remained unaltered in CNS and dLN of icKO mice (Fig. 2*B* and Fig. S6 *B-D*). Treg cell proportion was also normal at day 10 (Fig. S6*E*). The proportion of activated CD44^{high} CD62L^{low} Treg cells was unchanged in dLN and CNS between icKO and control mice (Fig. S7*A*). Also, Treg cells specific for the myelin oligodendrocyte glycoprotein 35-55 peptide $(MOG)_{35\text{-}55}$, the immunizing antigen in EAE, were present in similar proportions in icKO and control mice in both dLN and CNS (Fig. S7*B*). However, TNFR2-deficient Treg cells expressed lower levels of CTLA-4 and Blimp-1 in the CNS (Fig. 2 *C and D*), as observed in cKO mice. Once again, this altered Treg cell phenotype was not observed in the dLN, which is compatible with a disease control by TNFR2^{+} Treg cells in the inflamed CNS rather than in the dLN. Moreover, this suggests that TNFR2 was not involved in the initial activation steps but rather in the acquisition of an optimal immunosuppressive state by Treg cells after day 7.

To further address the mechanism of EAE exacerbation, we performed RNA-sequencing on Treg cells from the CNS and dLN of icKO and control mice at day 14. In the inflamed CNS, a number of important genes exhibited altered expression in mutant Treg cells (Fig. 2 *E and F*). For instance, the expression of several genes associated with the highly suppressive effector Treg cell subset, such as *Myb*, *Ccr8* and *Cd177* (25), was down-regulated in TNFR2-deficient Treg cells. Surprisingly, mRNA expression of *Ctla4* and *Prdm1* (Blimp-1) remained unchanged, suggesting

that TNFR2 ablation in Treg cells may lead to post-transcriptional modifications. Conversely, genes usually associated with Tconv cell effector function, such as granzymes and perforin, and even *Cd8a* and *Cd8b* genes, displayed augmented expression in mutant Treg cells. Gene set enrichment analyses (GSEA) revealed an enrichment of the $CD8^+$ Tconv cell signature in mutant Treg cells (Fig S8*A*). This was not due to cell contamination of the samples as mutant Treg cells expressed normal amounts of *Cd4* and *Zbtb7b* (ThPOK), as well as *Tbx21*, *Runx1 or Runx3*, compared to WT Treg cells (Fig. S8*B*). To confirm this data, some of the DEG were analyzed at protein level in the CNS. *CD8a*, *Thy1* (coding for CD90) and *Eomes* that had higher level of mRNA in TNFR2-deficient Treg cells (Fig. 8*C*), also displayed increased protein expression (Fig. S8*D*). Importantly, the increased CD8α expression was due to a slight shift of the whole Treg cell population and not to the presence of few cells expressing high level of CD8, definitively ruling out the hypothesis of the presence of $CD8^+$ Tconv cell contaminants. Interestingly, expression of the long non-coding RNA *Flicr*, which was described to negatively regulate *Foxp3* expression and Treg cell function (26), was increased in the absence of TNFR2. GSEA further confirmed that TNFR2-deficient Treg cells were less activated and did not acquire the full identity of Treg cells from the inflamed CNS, when compared with control Treg cells (Fig. 2*G***)**. Importantly, the differential expression of these genes in TNFR2-deficient Treg cells was not seen in dLNs, in which only subtle decrease in genes involved in homing such as *Ccr1*, *Itga5* or *Itgam* was observed (Fig. S9 *A and B***)**. Altogether, these results show that the loss of TNFR2 expression by Treg cells induces alteration of their activation and identity during EAE, specifically in the CNS and not in the dLN.

TNFR2 expression by Treg cells limits the activation and pathogenic function of Tconv cells in the CNS.

We then characterized the pathogenic profile of CD4 Tconv cells. Quite surprisingly, they acquired a similar $CD44^{high}$ $CD62L^{low}$ activated phenotype in icKO and control mice and expressed equivalent amounts of the pathogenic GM-CSF after strong polyclonal PMA ionomycin re-stimulation in dLN and CNS (Fig. S10 *A and B*). Also, MOG_{35-55} specific Tconv cells were present in similar proportions in both types of mice in dLN and CNS (Fig. S10*C*). More informative data were obtained when we performed transcriptomic analyses at day 14. In line with the aggravated EAE symptoms and the impairment of the Treg cell gene expression profile in icKO mice, transcriptomic analyses of $CD4^+$ Tconv cell counterparts in the CNS showed major alterations. The expression of 185 and 229 genes was respectively down- and up-regulated in Tconv cells isolated from mutant animals, compared to controls (Fig. 3*A*). Tconv cells from icKO mice displayed a highly activated phenotype. Notably, mRNA of cytokines and chemokines (*Csf2, Il22, Ifng, Tnf, Il2, Lta, Ccl3, Ccl4*) and cytokine receptors and chemokine receptors as well as other activation markers (*Il2ra*, *Il12r*, *Ifngr, Ccr2, Ccr5*, *Icos, Fasl, Ctla4, Gzmb*) were significantly increased in these cells (Fig. 3*B* and Fig. S9*C*). They also expressed increased levels of genes of signaling pathways (such as MAPK and NF-kB), interferon signature (*Ifit*, *Isg*) and transcription factors (*Prdm1, Bhlhe40, Rora, Egr1, Fosl2, Junb*), known to be up-regulated in activated T cells. Accordingly, the expression of genes characterizing resting T cells were down-regulated in Tconv cells from the CNS of icKO mice, such as *Sell* (CD62L), *Ly6c1*, *Ccr7*, *Klf2*, *Bach2*, *Tcf7* or *Lef1* (Fig. 3*B*). Among genes up-regulated in Tconv cells of icKO mice, network analysis of putative protein-protein interactions connected two nodes, one regrouping genes coding for activation markers with the other one belonging to an interferon signature. Interestingly, these two nodes were connected by the *Tnf* and *Ifng* genes (Fig. S9*D*). The metabolic profile icKO Tconv cells further supports their activated status with increased expression of most genes of the glycolytic pathway as well as of *Slc2a1* (Glut1), the main glucose transporter in T cells, and *Hif1a*, a master positive

202 regulator of glycolysis (Fig. 3*C* and Fig. S9*C*). GSEA analysis further confirmed that these icKO
203 Tconv cells had an activated status (Fig. 3*D*). Not only these Tconv cells have an activated status,
204 but also their transcriptome suggests a Th1/Th17 pathogenic profile with increased expression of
205 *Csf2* (GM-CSF), *Il22*, *Ifng*, *Ifngr* or *Il12r*. We confirmed some of these results at the protein level
206 by measuring cytokines produced by CNS-infiltrating cells isolated at day 14 by ELISA. GM-CSF,
207 which is the major pathogenic cytokine produced by Tconv cells in EAE (27), was significantly
208 increased in icKO mice compared to control mice after both anti-CD3 and immunizing myelin
209 antigen stimulation (Fig. 3*E*). IL-17A and IFN-γ production were slightly increased in icKO Tconv
210 cells as well but not significantly. All these modified expression patterns (gene expression and
211 cytokine expression) were not observed -or at a much lower extend- in the dLN (Fig. S9 *E*-*G*).
212 Altogether, these data strongly suggest that TNFR2 expression by Treg cells is involved in the local
213 suppression of activated and pathogenic Tconv cells in the CNS after disease onset, but not in their
214 initial priming in lymphoid tissues.
215
216 **TNF/TNR2 signaling in Treg cells enables local suppression of EAE in the inflamed CNS.**
217 We then conducted experiments to further confirm the CNS-restricted role of TNFR2-expressing
218 Treg cells. In the course of active EAE, the disease is initiated in dLN and spleen. Then, from day
219 5, pathogenic Tconv cells migrate to the CNS where they are re-activated, leading to their
220 progressive accumulation and increased inflammation, perpetuating locally the disease process
221 (28). We first analyzed the phenotype of T cells during priming in lymphoid tissues to evaluate
222 their capacity to acquire pathogenic features. We assessed expression of CD11a (LFA-1 α chain),
223 CXCR3, CCR6 and CD49d (VLA-4 α chain) because of their involvement in T cell migration from
224 lymphoid tissues to inflamed CNS during EAE (29, 30). Ten days after EAE induction, these

225 molecules were expressed at the same levels in control and cKO mice, suggesting unaltered
226 migration capacity into the CNS (Fig. S11). To more directly quantify priming of MOG-reactive
227 T cells, we transferred T-cell receptor-transgenic Tconv cells specific for this antigen in cKO and
228 control mice. Then, mice were immunized with MOG_{35-55} peptide and we measured the activation
229 of donor cells in dLN and spleen 3 and 7 days later. The level of T-cell proliferation and expansion
230 was high and comparable in the 2 groups of mice (Fig. 4*A* and Fig. S12 *A* and *B*). Donor MOG-
231 specific T cells expressed similar levels of CD11a and CD49d and of the IFNγ, IL-17A and GM-
232 CSF pathogenic cytokines after PMA-ionomycine stimulation in cKO mice compared to controls
233 (Fig. S12 *C and D*). Together with the unchanged proportions of MOG-reactive T cells we detected
234 in icKO animals (Fig. S10*C*), these data suggest a normal priming of MOG-specific Tconv cells in
235 lymphoid tissues in both cKO and icKO mice. To further assess the pathogenicity of polyclonal
236 MOG-specific T-cells primed in dLN, we measured their capacity to induce EAE after adoptive
237 transfer in naive mice. Remarkably, cells primed in cKO and control mice, and re-stimulated ex
238 vivo, induced similar passive EAE (Fig. 4*B*). Thus, all these data concur to show that exacerbation
239 of EAE in cKO mice was not due to enhanced initial priming of MOG-specific T cells in spleen
240 and dLN. Then, to further confirm that TNFR2-expressing Treg cells selectively controlled EAE
241 severity within the inflamed CNS, we transferred WT pathogenic T cells to cKO or control naive
242 mice. In this setting, injected cells rapidly migrated into the CNS to damage the neural tissue during
243 passive EAE, without being primed in the dLN. Strikingly, EAE was much more severe in cKO
244 than control recipients (Fig. 4*C*). We obtained similar findings when we transferred pathogenic T-
245 cells in WT recipients that were treated with an anti-TNF blocking mAb (Fig. 4*D*). Taken together,
246 these results confirm our earlier findings that TNFR2 signaling in Treg cells is critical to control
247 EAE within the inflamed CNS, rather than limiting the priming of pathogenic T-cells in lymphoid
248 tissues.

Systemic modulation of the TNF/TNFR2 axis affects EAE severity.

The protective facet of TNF in CNS autoimmunity relied originally on observations made in patients. Indeed, anti-TNF therapies are formally contra-indicated in MS patients because of disease exacerbation (31, 32). The mechanism of this long-term conundrum, well known to clinicians, remains essentially unexplained. To investigate if our earlier findings could bring a mechanistic insight to this adverse effect of anti-TNF treatments, we assessed the effect of this therapy on EAE severity and Treg cell phenotype in EAE. WT mice were treated with a blocking anti-TNF mAb from day 10 - a time when they developed the first clinical signs - until day 18. As observed in MS patients, these mice exhibited an aggravated form of EAE compared to isotype-control treated mice (Fig. 5*A*)**.** Similar findings were obtained when using the clinically approved soluble TNFR2-Fc fusion receptor (Etanercept) to block TNF (Fig. 5*B*). Interestingly, TNF-blockade at earlier time points (from day 0) did not significantly modify the course of the disease (Fig. 5*C*)**,** highlighting once more the protective role of TNF during established disease and not during Tconv cell priming. We next analyzed the Treg cell compartment in the inflamed CNS of these mice. In anti-TNF treated mice, Treg cell proportion was significantly reduced in the CNS compared to control animals, whereas it was unchanged in dLN. These observations are similar to the ones we previously made in TNFR2 conditional KO mice and, which further support the CNS-restricted role of TNF on Treg cells (Fig. 5*D*). This protective effect of TNF was most likely due to TNFR2 triggering since blocking this receptor with a specific mAb worsened EAE (Fig. 5*E*), similarly to anti-TNF mAb treatment or TNFR2 ablation in Treg cells. Finally, in a therapeutic perspective, we investigated whether stimulating TNFR2 signaling in the course of the disease could improve disease outcome. Remarkably, the use of a TNFR2 specific agonist from day 4 to 18 significantly reduced EAE severity (Fig. 5*F*). This therapeutic effect was lost in icKO animals,

suggesting that this agonist functions by stimulating TNFR2-expressing Treg cells (Fig. S13). Collectively, these data are in line with our previous findings, highlighting the protective role of TNF in CNS during EAE and providing a mechanistic explanation for the deleterious events following anti-TNF administration in patients with MS.

DISCUSSION

The protective properties of Treg cells in autoimmune diseases are clearly established. However, when and where do endogenous Treg cells control these diseases remain unknown. Some published works provided indirect evidence that Treg cells may suppress an autoimmune disease in the target organ. Indeed, late accumulation of Treg cells was observed in the inflamed CNS during EAE (6, 33, 34). Systemic Treg cell deletion precipitated established autoimmune diseases but at the expense of massive and multifocal inflammation, precluding a proper evaluation of physiological function of Treg cells (6, 35). Administration of Treg cells specific for the target tissue had a therapeutic efficacy in organ-specific autoimmune diseases, suggesting a capacity to suppress pathogenic cells locally (36, 37). However, these studies did not address the role of endogenous Treg cells during the natural course of the disease. Here, we found that TNFR2 ablation in Treg cells after EAE induction had no systemic impact, but led to increased CNS inflammation and disease severity. This suggested that Treg cells suppressed EAE at peak of disease in the inflamed CNS and not during T-cell priming in the dLN. This hypothesis was further supported by the following cumulative proofs. (i) Treg cell phenotype, and their proportion in some models, were altered in the CNS but not in the dLN in cKO mice, icKO mice or WT mice treated with anti-TNF drugs. (ii) Increased expression of activation molecules and pathogenic GM-CSF by Tconv cells could be observed in the CNS of icKO mice but not in dLN. The increased production of GM-CSF in icKO mice was no longer observed after PMA-ionomycin stimulation, probably because this strong and non-physiological activation could outweigh the difference observed with more physiological T cell receptor stimulation. (iii) Activation and expansion in lymphoid tissues and migration into the CNS of polyclonal and MOG-specific T cells appeared normal in cKO and icKO mice, as compared to control mice. (iv) Blocking TNF in WT mice from day 10, but not from day 0, after disease induction led to EAE exacerbation, suggesting that the early autoimmune process

303 that was primed in dLN was not altered by the absence of TNFR2 in Treg cells. In the same line,
304 disease exacerbation following TNFR2 ablation in Treg cells was obtained when this deletion
305 obtained by tamoxifen administration was performed 7 days after disease induction. (v) Cell
306 transfer experiments showed that the activation of myelin-specific T-cells in spleen and dLN, as
307 well as their capacity to induce passive EAE, were largely similar in cKO and control mice.
308 However, it remains possible that the ex vivo re-stimulation protocol, which is required to induce
309 disease, may have skewed the potential differences between Tconv cells from the two strains. (vi)
310 Finally, pathogenic T cells from WT mice that were re-activated in the CNS after their injection
311 induced a more severe disease in cKO than in control recipients. Thus, the control of EAE by
312 TNFR2-expressing Treg cells is regulated in the inflamed CNS and not in the dLN. Together, our
313 work strongly supports the concept that endogenous Treg cells suppress an autoimmune disease in
314 the target tissue.
315 Our findings also provide some insight into the mechanism of EAE control by Treg cells in the
316 CNS. Indeed, TNFR2 expression by Treg cells appears to control their function rather than their
317 numbers. We did find a decreased proportion of Treg cells in the CNS at day 10 in cKO mice but
318 this was no more observed earlier (day 7) or later (day 15) in these mice or in the icKO animals.
319 More importantly, TNFR2-deficient Treg cells have lower mRNA expression of several Treg cell-
320 signature genes and increased expression of genes normally expressed by Tconv cells. Also,
321 TNFR2-deficient Treg cells expressed lower level of *Myb* that was shown to be essential for
322 differentiation of effector Treg cells (25). The lack of TNFR2 expression in Treg cells seems to
323 have an additional impact on protein expression, as observed for CTLA-4 and Blimp-1, whose
324 protein levels were decreased in CNS of icKO mice. This may alter Treg cell suppressive activity,
325 as CTLA-4 is one of the major mechanisms of Treg cell-mediated suppression and Blimp-1 is
326 critical to promote IL-10 production (1, 23, 24). Also, Blimp-1 is expressed by the fraction of

highly suppressive effector Treg cells and is up-regulated in CNS Treg cells during EAE. Moreover, its ablation in Treg cells led to exacerbated EAE, reduced Treg cell identity and increased expression of inflammatory cytokines, such as IL-17 (2, 3). Consequently, TNFR2-deficient Treg cells would be deficient in suppressing Tconv cells in the CNS, leading to massive Tconv cell activation, as observed at the level of activation markers, cytokines and chemokines, signaling molecules, transcription factors and glucose metabolism. These highly activated Tconv cells produced increased level of pathogenic cytokines such as GM-CSF, precipitating EAE. In conclusion, our data demonstrate that TNFR2 expression by Treg cells is essential to limit EAE severity by promoting their transient expansion and by increasing their suppressive function in the CNS, thereby limiting pathogenic Tconv cell activation. Thus, we reveal here a non-redundant function of TNF in the control of EAE in the inflamed CNS. Recent findings emphasized the critical role of IL-33 in the accumulation of Treg cells residing in the intestine or adipose tissues (38-40). Thus, depending on the tissue and type of inflammation, Treg cells may rely on different environmental cues (IL-33, TNF) for their homeostasis and function.

Besides this non-redundant function of TNFR2 in Treg cells, our data also bring a mechanistic explanation to the deleterious effect of TNF-blockade in patients with MS. A series of pre-clinical studies in mice conducted in the nineties concluded that blocking TNF was beneficial in EAE (reviewed in (41)). These findings led to initiate two clinical trials in MS patients that had to be rapidly stopped because of disease aggravation (31, 32). Here, we revisited this question using reagents that selectively blocks TNF, whereas older studies used drugs blocking both TNF and lymphotoxin-α, which is an issue since the latter cytokine is pathogenic in EAE (42). We found that blocking TNF at disease's peak induced EAE exacerbation, as in MS patients who were also treated during advanced disease progression. Interestingly, when TNF was blocked at earlier times, EAE was not exacerbated, and even slightly delayed. Thus, at disease initiation, TNF might be

pathogenic by activating antigen-presenting cells via TNFR1, whereas it would regulate the disease afterwards, by activating Treg cells via TNFR2 in the inflamed CNS. In this line, blocking TNFR1 at disease induction attenuated EAE (43), whereas we showed that blocking TNFR2 at day 10 induced disease exacerbation, similarly to late TNFR2 ablation in Treg cells. Furthermore, we demonstrated that stimulation of TNFR2 signaling reduced EAE severity.

In conclusion, our data reveal that the TNF/TNFR2 axis is critical to reach an optimal Treg cell function specifically in the CNS during EAE, thereby preventing excessive inflammation and controlling disease severity. Moreover, our results bring new insights in the mechanism of autoimmune disease control by Treg cells and provide an explanation for the failure of anti-TNF therapy in MS patients, paving the way to the development of more specific treatments aiming at the selective blockade of TNFR1 and/or selective stimulation of TNFR2.

METHODS

Mice. C57BL/6J (WT) mice were purchased from Janvier Labs (France). *Tnfrsf1b*$^{tm1Mwm/}$J (*Tnfrs1b*$^{-/-}$), *Foxp3*$^{tm9(EGFP/cre/ERT2)Ayr}$/J (*Foxp3*$^{Cre\text{-}ERT2}$) and C57BL/6 Tg(Tcra2D2,Tcrb2D2)1Kuch/J (2D2) T cell receptor transgenic mice, specific for myelin oligodendrocyte glycoprotein, were purchased from the Jackson Laboratory. *Cd3*^{etm1Mal} (*Cd3*$^{-/-}$), CD45.1 and CD90.1 mice were provided by the Cryopreservation Distribution Typing and animal Archiving department (Orléans, France). B6.129(Cg)-*Foxp3*$^{tm4(YFP/icre)Ayr}$/J (*Foxp3*^{Cre}) mice were a gift from Pr. Alexander Rudensky. C57BL/6-*Tnfrsf1b*$^{<tm1c(EUCOMM)Wtsi>}$/Ics (*Tnfrsf1b*^{fl}) mice were obtained from the EMMA consortium. All mice were on a C57BL/6J background or have been backcrossed at least 10 times to C57BL/6J mice. Mice were housed under specific pathogen-free conditions and were studied at 7–14 weeks of age or two months after bone marrow transplanted.

TNF- and TNFR2-targeting biological. Anti-TNF (XT3-11) and anti-TNFR2 (TR75-54.7) mAb were purchased from BioXCell and were injected at a dose of 500 μg by intraperitoneal route every other day for 8 or 14 days. Etanercept (TNFR2-Fc) was provided by Wyeth and was administered at a dose of 1 mg by intraperitoneal route every other day for 8 days. Purification and functional characterization of the TNFR2-specific agonist STAR2 has been described elsewhere (10).

Bone marrow transplantation. Bone marrow cells were isolated from tibia and femur of donor mice. Recipient mice were lethally irradiated (10.5 Gray) and transplanted intravenously with 10 x 10^6 bone marrow cells. EAE was induced at least 8 weeks after transplantation.

EAE induction. For active EAE, mice were injected subcutaneously in the flanks with 100 µg of MOG_{35-55} peptide (Polypeptide) emulsified in 100 µl of complete Freund adjuvant (Sigma-Aldrich) supplemented with 50 µg of heat-killed *Mycobacterium tuberculosis* H37Ra (BD Biosciences). Animals were additionally injected intravenously with 200 ng of *Bordetella pertussis* toxin (Enzo) at the time of immunization and two days later. For the passive EAE model, we first induced active EAE in donor mice as described above to generate pathogenic cells. Ten days post-immunization, cells from spleen and dLN were cultured in complete RPMI (Gibco) medium with 10% fetal calf serum at 5 x 10^6 cells/ml with 20 µg/ml of MOG_{35-55} peptide, 10 µg/ml of anti-IFNγ (XMG1.2, BioXCell) and 5 ng/ml of IL-23 (R&D Systems). After 3 days, dead cells were removed with a Ficoll gradient and 2 x 10^6 cells were injected intravenously to recipient mice to induce passive EAE. The clinical evaluation was performed on a daily bases by a 6-point scale ranging: 0, no clinical sign; 1, limp tail; 2, limp tail, impaired righting reflex, and paresis of one limb; 3, hind limb paralysis; 4, hind limb and forelimb paralysis; 5, moribund/death. A score of 5 was permanently attributed to dead animals.

Preparation of cell suspensions. For isolation of CNS-infiltrating leukocytes, mice were anesthetized with a xylazine/ketamine solution and perfused with cold PBS. Spinal cords were removed by intrathecal hydrostatic pressure. Brain and spinal cords were cut into small pieces and digested in RPMI 1640 (Gibco) supplemented with 1 mg/ml collagenase type IV (Sigma), 100 µg/ml DNase I (Sigma) and 1 µg/ml TLCK for 30 min at 37°C followed by mechanical desegregation. Single cell suspensions were washed once and re-suspended in Percoll 40%. For FACS analysis, cells were laid on a Percoll 80% solution, centrifuged for 20 min at 2,000 rpm at room and mononuclear cells were collected from the interface of the 40:80% Percoll gradient and were washed two times in a PBS-3% fetal calf serum buffer. For FACS cell sorting, cells were

centrifuged for 10 minutes at 400g and mononuclear cells were collected from the pellet of the monolayer Percoll gradient. Cells from thymus, spleen and LN were obtained after mechanical dilacerations.

Antibodies and flow cytometry analysis. The mAb and fluorescent reagents used in this study are listed below in the table. Intracellular staining was performed using the Foxp3/Transcription Factor Staining Buffer Set kit and protocol from eBioscience. Identification of MOG-specific T cells was performed using the I-A(b) mouse MOG 38-49 GWYRSPFSRVVH APC-labeled tetramer, obtained from the NIH Tetramer Facility, according to their protocol. Intracellular cytokine staining (Fig S5, S10 and S12) was assessed after 4 hours of PMA (25 ng/ml) ionomcycin (1 mg/ml) stimulation in RPMI 1640 containing 10% FCS and Golgi plug (BD Biosciences). Cells were acquired on a BD LSRII cytometer and analyzed using the FlowJo software.

mAb or reagent	Clone	Vendor	Reference	Dilution
BV510 anti-mouse CD4	RM4-5	BD Biosciences	563106	1/500
BUV496 anti-mouse CD4	GK1.5	BD Biosciences	564667	1/400
Alexa Fluor® 700 anti-mouse CD8a	53-6.7	BD Biosciences	557959	1/400
BUV805 anti-mouse CD8a	53-6.7	BD Biosciences	564920	1/400
PerCP-C5.5 anti-mouse CD11a	2D7	BD Biosciences	562809	1/100
Biotin anti-mouse CD25	7D4	BD Biosciences	553070	1/300
PE-Cy7 anti-mouse CD44	IM7	Invitrogen/eBioscience	25-0441-82	1/400
BUV395 anti-mouse CD45	30-F11	BD Biosciences	564279	1/400
PE-CF594 anti-mouse CD45	30-F11	BD Biosciences	562420	1/1000
PE anti-mouse CD45.1	A20	BD Biosciences	561872	1/100
Biotin anti-mouse CD45.1	A20	Miltenyi	130101902	1/10
PE anti-mouse CD49d	R1-2	BD Biosciences	553157	1/100
AF700 anti-mouse CD62L	MEL-14	BD Biosciences	560517	1/100
APC anti-mouse CD90.1	OX-7	BD Biosciences	561409	1/400
PE-Cy7 anti-mouse ICOS	7E.17G9	Invitrogen/eBioscience	25-9942-82	1/400
PE anti-mouse CTLA-4 (CD152)	UC104F10-11	BD Biosciences	553720	1/200
Alexa Fluor® 647 anti-mouse Blimp1	5E7	BD Biosciences	563643	1/100
PE-Cy7 anti-mouse Eomes	Dan11mag	Invitrogen/eBioscience	25-4875-80	1/100
BV421 anti-mouse TNFR2 (CD120b)	TR75-89	BD Biosciences	564088	1/200

FITC anti-mouse GITR	DTA-1	BD Biosciences	558139	1/200
PE anti-mouse Vβ11	RR3-15	BD Biosciences	553198	1/200
BV421 anti-mouse CCR6	140706	BD Biosciences	564736	1/20
APC anti-mouse CXCR3	CXCR3-173	BD Biosciences	562266	1/100
APC anti-human/mouse Foxp3	FJK-16s	Invitrogen/eBioscience	17-5773-82	1/200
FITC anti-human/mouse Foxp3	FJK-16s	Invitrogen/eBioscience	11-5773-82	1/200
PE-e610 anti-huma/mouse Foxp3	FJK-16s	Invitrogen/eBioscience	61-5773-82	1/100
eF450 anti mouse/human Ki67	SOLA15	Invitrogen/eBioscience	48-5698-82	1/400
AF647 anti-mouse IFNg	XMG1.2	BD Biosciences	557735	1/100
APC-Cy7 anti-mouse IL-17A	TC11-18H10	BD Biosciences	560821	1/100
PE anti-mouse GM-CSF	MP1-22E9	BD Biosciences	554406	1/100
BV421 Streptavidin		BD Biosciences	563259	1/400
PE-Cy7 Steptavidin		Invitrogen/eBioscience	25-4317-82	1/200
e450 Cell trace		Life technologies		1/2000
e506 Fixable viability dye		Invitrogen/eBioscience	65-0866-14	1/1000

Treg and Tconv cell purification. For suppression assay, colitis and transcriptomic analyses, cell suspensions from the spleen, LN or the CNS were stained with e780 viability dye, BV510 anti-CD4 (RM4-5) and PE-CF594 anti-CD45 (30F11) mAbs. Purified Tconv cells ($CD4^+YFP^-$ or $CD4^+GFP^-$) and Treg cells ($CD4^+YFP^+$ or $CD4^+GFP^+$) were obtained using a BD FACSAria II. For transcriptomic analyses, cells were sorted twice with the cytometer leading to over 99.8% purity.

Cell culture. Culture medium was composed of RPMI 1640 (Gibco) supplemented with 10% fetal calf serum. For suppression assay, purified Tconv cells (2.5 x 10^4 cells/well), labeled with CellTrace Violet (Proliferation Kit, Life technologies), and purified Treg cells were stimulated by splenocytes from *Cd3*$^{-/-}$ mice (7.5 x 10^4 cells/well) and soluble anti-CD3 mAb (0.05 µg/ml 2C11, BioXCell) in 96-well plate at different Treg/Tconv cell ratios. At day 3, CellTrace dilution was assessed by flow cytometry. To assess TNFR2 expression, whole splenocytes (3 x 10^6 cells/well) were stimulated by soluble anti-CD3 (5 µg/ml 2C11, BioXCell) in 96-well plate. For ELISA studies (Fig. 3, S9), cells from 3.5 x 10^6 LN cells in 2 ml in 24-well plates or 1 x 10^5 CNS cells in 200 µl

in 96-round bottom well plates were stimulated with 10 or 100 µg/ml of MOG or with 5 µg/ml of anti-CD3 mAb (2C11) for 24h (CNS cells) or 72h (LN cells) before performing ELISA on the supernatant using kits from Invitrogen.

Adoptive transfer of 2D2 T cells. LN and spleen cells from 2D2 CD90.1 or 2D2 CD45.1 mice were stained incubated with anti-CD19 (6D5), anti-CD11b (M1/70), anti-CD11c (N418), anti-CD8 (53-6.7) and anti-CD25 (7D4) biotin-labeled mAbs and then were coated with anti-biotin microbeads (Miltenyi Biotec). After magnetic sorting, cells of the $CD4^+$ enriched negative fraction were labeled with CellTrace Violet Proliferation Kit and were intravenously injected in naive mice (10^6 cells/mouse). The following day, mice were immunized with MOG_{35-55} peptide as for EAE induction. Donor cells, identified by their $CD4^+CD90.1^+V\beta11^+$ (T cell receptor transgene) or $CD45.1^+CD3^+$ phenotypes, were analyzed by flow cytometry in dLNs and spleen 3 or 7 days later.

RNA-sequencing and bioinformatics analyses. RNA was extracted from highly purified Treg and Tconv cells using the NucleoSpin RNA XS kit from Macherey-Nagel, quantified using a ND-1000 NanoDrop spectrophotometer (NanoDrop Technologies) and purity/integrity was assessed using disposable RNA chips (Agilent High Sensitivity RNA ScreenTape) and an Agilent 2200 Tapestation (Agilent Technologies, Waldbrunn, Germany). mRNA library preparation was performed following manufacturer's recommendations (SMART-Seq v4 Ultra Low Input RNA Kit TAKARA). Final-17 samples pooled library prep was sequenced on Nextseq 500 ILLUMINA with HighOutPut cartridge (2x400Millions of 75 bases reads), corresponding to 2 times 23 x 10^6 reads per sample after demultiplexing. Poor quality sequences have been trimmed or removed with Trimmomatic software to retain only good quality paired reads. Star v2.5.3a (44) has been used to

align reads on reference genome mm10 using standard options. Quantification of gene and isoform abundances has been done with rsem 1.2.28 (45) prior to normalization on library size with DESEq2 bioconductor package. Finally, differential analysis has been conducted with edgeR bioconductor package. Multiple hypothesis adjusted p-values were calculated with the Benjamini-Hochberg procedure to control FDR. For Treg cells, data were obtained from a biological triplicate. For Tconv cells, data were obtained from two independent experiments with biological quadruplicate, after exclusion of two outliers. GSEA has been done with fGSEA bioconductor R package (v1.12.0) on pre-ranked list. Genes in our data set (GSE165821) were ranked according to the signed fold-change multiplied by the -log10 p-value of the differential analysis. Gene sets were extracted from GSE165821 (Fig. 2G, right panel), GSE146135 (Fig. 2G, left panel) and GSE11057 (Fig. 3D).

Statistics. Statistical analyses were performed using GraphPad Prism Software v8.3.1. For EAE scores and 2-groups comparisons, statistical significance was determined using the two-tailed unpaired nonparametric Mann–Whitney U-test, excluding D0 to D5 as all scores were 0. For survival curves, Log-Rank (Mantel-Cox) test was used. For ELISA assays, 2-way unpaired ANOVA test with Sidak correction for multiple comparisons was used. *p<0.05, **p<0.01, ***p<0.001, ****p<0.0001.

Study approval. All experimental protocols were approved by the "Comité d'éthique en expérimentation animal Charles Darwin N◦5" under the number 02811.03 and are in compliance with European Union guidelines.

Data Availability Statement: The RNA-Seq data reported in this paper have been deposited in the Gene Expression Omnibus (GEO) database, https://www.ncbi.nlm.nih.gov/ geo (accession no. GSE165821).

ACKNOWLEDGMENTS

This work was supported by the Agence Nationale de la Recherche (ANR-09-GENO-006-01, ANR-15-CE15-0015-03), the Fondation pour la Recherche Médicale (équipe FRM), the Fondation Bettencourt Schueller to BLS, the Association de la Recherche sur la Sclérose en Plaques to BLS and YGB, the ATIP-Avenir young investigator program to YGB, and by the Deutsche Forschungsgemeinschaft (324392634 –TRR 221, WA 1025/31-1) to HW.

We are grateful to Prof. Alexander Rudensky for providing us with the Foxp3Cre mice, to Prof. Jeffrey Bluestone and Matthew Krummel for critical reading of the manuscript, to Dr. Lennart Mars for providing us with the 2D2 mice and to Doriane Foret, Flora Issert, Olivier Bregerie and Maria Mihoc for their expert care of the mouse colony. We thank the NIH Tetramer Facility for providing us with the MOG tetramer. We thank the great expertise of Yannick Marie, Delphine Bouteiller, Beata Gyorgy and Justine Guegan from the bio-informatic plateform of the Institut du Cerveau et de la Moelle Epinière (Paris).

DECLARATION OF INTERESTS

The authors declare no competing interests.

REFERENCES

1. Cretney E*, et al.* (2011) The transcription factors Blimp-1 and IRF4 jointly control the differentiation and function of effector regulatory T cells. *Nat Immunol* 12:304-311.
2. Garg G*, et al.* (2019) Blimp1 Prevents Methylation of Foxp3 and Loss of Regulatory T Cell Identity at Sites of Inflammation. *Cell Rep* 26:1854-1868 e1855.
3. Ogawa C*, et al.* (2018) Blimp-1 Functions as a Molecular Switch to Prevent Inflammatory Activity in Foxp3(+)RORgammat(+) Regulatory T Cells. *Cell Rep* 25:19-28 e15.
4. Josefowicz SZ, Lu LF, & Rudensky AY (2012) Regulatory T cells: mechanisms of differentiation and function. *Annu Rev Immunol* 30:531-564.
5. Wing JB, Tanaka A, & Sakaguchi S (2019) Human FOXP3(+) Regulatory T Cell Heterogeneity and Function in Autoimmunity and Cancer. *Immunity* 50:302-316.
6. McGeachy MJ, Stephens LA, & Anderton SM (2005) Natural recovery and protection from autoimmune encephalomyelitis: contribution of CD4+CD25+ regulatory cells within the central nervous system. *J Immunol* 175:3025-3032.
7. Kohm AP, Carpentier PA, Anger HA, & Miller SD (2002) Cutting edge: CD4+CD25+ regulatory T cells suppress antigen-specific autoreactive immune responses and central nervous system inflammation during active experimental autoimmune encephalomyelitis. *J Immunol* 169:4712-4716.
8. Hori S, Haury M, Coutinho A, & Demengeot J (2002) Specificity requirements for selection and effector functions of CD25+4+ regulatory T cells in anti-myelin basic protein T cell receptor transgenic mice. *Proc Natl Acad Sci U S A* 99:8213-8218.
9. Chen X, Baumel M, Mannel DN, Howard OM, & Oppenheim JJ (2007) Interaction of TNF with TNF receptor type 2 promotes expansion and function of mouse CD4+CD25+ T regulatory cells. *J Immunol* 179:154-161.

10. Chopra M, *et al.* (2016) Exogenous TNFR2 activation protects from acute GvHD via host T reg cell expansion. *J Exp Med* 213:1881-1900.

11. Grinberg-Bleyer Y, *et al.* (2010) Pathogenic T cells have a paradoxical protective effect in murine autoimmune diabetes by boosting Tregs. *J Clin Invest* 120:4558-4568.

12. Leclerc M, *et al.* (2016) Control of GVHD by regulatory T cells depends on TNF produced by T cells and TNFR2 expressed by regulatory T cells. *Blood* 128:1651-1659.

13. Zaragoza B, *et al.* (2016) Suppressive activity of human regulatory T cells is maintained in the presence of TNF. *Nat Med* 22:16-17.

14. Yang S, *et al.* (2019) Differential roles of TNFalpha-TNFR1 and TNFalpha-TNFR2 in the differentiation and function of CD4(+)Foxp3(+) induced Treg cells in vitro and in vivo periphery in autoimmune diseases. *Cell Death Dis* 10:27.

15. Atretkhany KN, *et al.* (2018) Intrinsic TNFR2 signaling in T regulatory cells provides protection in CNS autoimmunity. *Proc Natl Acad Sci U S A* 115:13051-13056.

16. Probert L, *et al.* (2000) TNFR1 signalling is critical for the development of demyelination and the limitation of T-cell responses during immune-mediated CNS disease. *Brain* 123 (Pt 10):2005-2019.

17. Suvannavejh GC, *et al.* (2000) Divergent roles for p55 and p75 tumor necrosis factor receptors in the pathogenesis of MOG(35-55)-induced experimental autoimmune encephalomyelitis. *Cell Immunol* 205:24-33.

18. Tsakiri N, Papadopoulos D, Denis MC, Mitsikostas DD, & Kollias G (2012) TNFR2 on non-haematopoietic cells is required for Foxp3+ Treg-cell function and disease suppression in EAE. *Eur J Immunol* 42:403-412.

19. Becher B, Waisman A, & Lu LF (2018) Conditional Gene-Targeting in Mice: Problems and Solutions. *Immunity* 48:835-836.

20. Kurachi M, Ngiow SF, Kurachi J, Chen Z, & Wherry EJ (2019) Hidden Caveat of Inducible Cre Recombinase. *Immunity* 51:591-592.

21. Bittner-Eddy PD, Fischer LA, & Costalonga M (2019) Cre-loxP Reporter Mouse Reveals Stochastic Activity of the Foxp3 Promoter. *Front Immunol* 10:2228.

22. Franckaert D*, et al.* (2015) Promiscuous Foxp3-cre activity reveals a differential requirement for CD28 in Foxp3(+) and Foxp3(-) T cells. *Immunol Cell Biol* 93:417-423.

23. Wing K*, et al.* (2008) CTLA-4 control over Foxp3+ regulatory T cell function. *Science* 322:271-275.

24. Neumann C*, et al.* (2014) Role of Blimp-1 in programing Th effector cells into IL-10 producers. *J Exp Med* 211:1807-1819.

25. Dias S*, et al.* (2017) Effector Regulatory T Cell Differentiation and Immune Homeostasis Depend on the Transcription Factor Myb. *Immunity* 46:78-91.

26. Zemmour D, Pratama A, Loughhead SM, Mathis D, & Benoist C (2017) Flicr, a long noncoding RNA, modulates Foxp3 expression and autoimmunity. *Proc Natl Acad Sci U S A* 114:E3472-E3480.

27. Codarri L*, et al.* (2011) RORgammat drives production of the cytokine GM-CSF in helper T cells, which is essential for the effector phase of autoimmune neuroinflammation. *Nat Immunol* 12:560-567.

28. Bailey SL, Schreiner B, McMahon EJ, & Miller SD (2007) CNS myeloid DCs presenting endogenous myelin peptides 'preferentially' polarize CD4+ T(H)-17 cells in relapsing EAE. *Nat Immunol* 8:172-180.

29. Sallusto F*, et al.* (2012) T-cell trafficking in the central nervous system. *Immunol Rev* 248:216-227.

30. Sporici R & Issekutz TB (2010) CXCR3 blockade inhibits T-cell migration into the CNS during EAE and prevents development of adoptively transferred, but not actively induced, disease *Eur J Immunol* 40:2751-2761.

31. Study-group (1999) TNF neutralization in MS: results of a randomized, placebo-controlled multicenter study. The Lenercept Multiple Sclerosis Study Group and The University of British Columbia MS/MRI Analysis Group. *Neurology* 53:457-465.

32. van Oosten BW*, et al.* (1996) Increased MRI activity and immune activation in two multiple sclerosis patients treated with the monoclonal anti-tumor necrosis factor antibody cA2. *Neurology* 47:1531-1534.

33. Korn T*, et al.* (2007) Myelin-specific regulatory T cells accumulate in the CNS but fail to control autoimmune inflammation. *Nat Med* 13:423-431.

34. O'Connor RA, Malpass KH, & Anderton SM (2007) The inflamed central nervous system drives the activation and rapid proliferation of Foxp3+ regulatory T cells. *J Immunol* 179:958-966.

35. Feuerer M, Shen Y, Littman DR, Benoist C, & Mathis D (2009) How punctual ablation of regulatory T cells unleashes an autoimmune lesion within the pancreatic islets. *Immunity* 31:654-664.

36. Stephens LA, Malpass KH, & Anderton SM (2009) Curing CNS autoimmune disease with myelin-reactive Foxp3+ Treg. *Eur J Immunol* 39:1108-1117.

37. Tang Q*, et al.* (2004) In vitro-expanded antigen-specific regulatory T cells suppress autoimmune diabetes. *J Exp Med* 199:1455-1465.

38. Schiering C*, et al.* (2014) The alarmin IL-33 promotes regulatory T-cell function in the intestine. *Nature* 513:564-568.

599 39. Kolodin D*, et al.* (2015) Antigen- and cytokine-driven accumulation of regulatory T cells
600 in visceral adipose tissue of lean mice. *Cell Metab* 21:543-557.
601 40. Vasanthakumar A*, et al.* (2015) The transcriptional regulators IRF4, BATF and IL-33
602 orchestrate development and maintenance of adipose tissue-resident regulatory T cells. *Nat*
603 *Immunol* 16:276-285.
604 41. Dendrou CA, Bell JI, & Fugger L (2013) A clinical conundrum: the detrimental effect of
605 TNF antagonists in multiple sclerosis. *Pharmacogenomics* 14:1397-1404.
606 42. Suen WE, Bergman CM, Hjelmstrom P, & Ruddle NH (1997) A critical role for
607 lymphotoxin in experimental allergic encephalomyelitis. *J Exp Med* 186:1233-1240.
608 43. Williams SK*, et al.* (2014) Antibody-mediated inhibition of TNFR1 attenuates disease in a
609 mouse model of multiple sclerosis. *PLoS One* 9:e90117.
610 44. Dobin A*, et al.* (2013) STAR: ultrafast universal RNA-seq aligner. *Bioinformatics* 29:15-
611 21.
612 45. Li B & Dewey CN (2011) RSEM: accurate transcript quantification from RNA-Seq data
613 with or without a reference genome. *BMC Bioinformatics* 12:323.
614

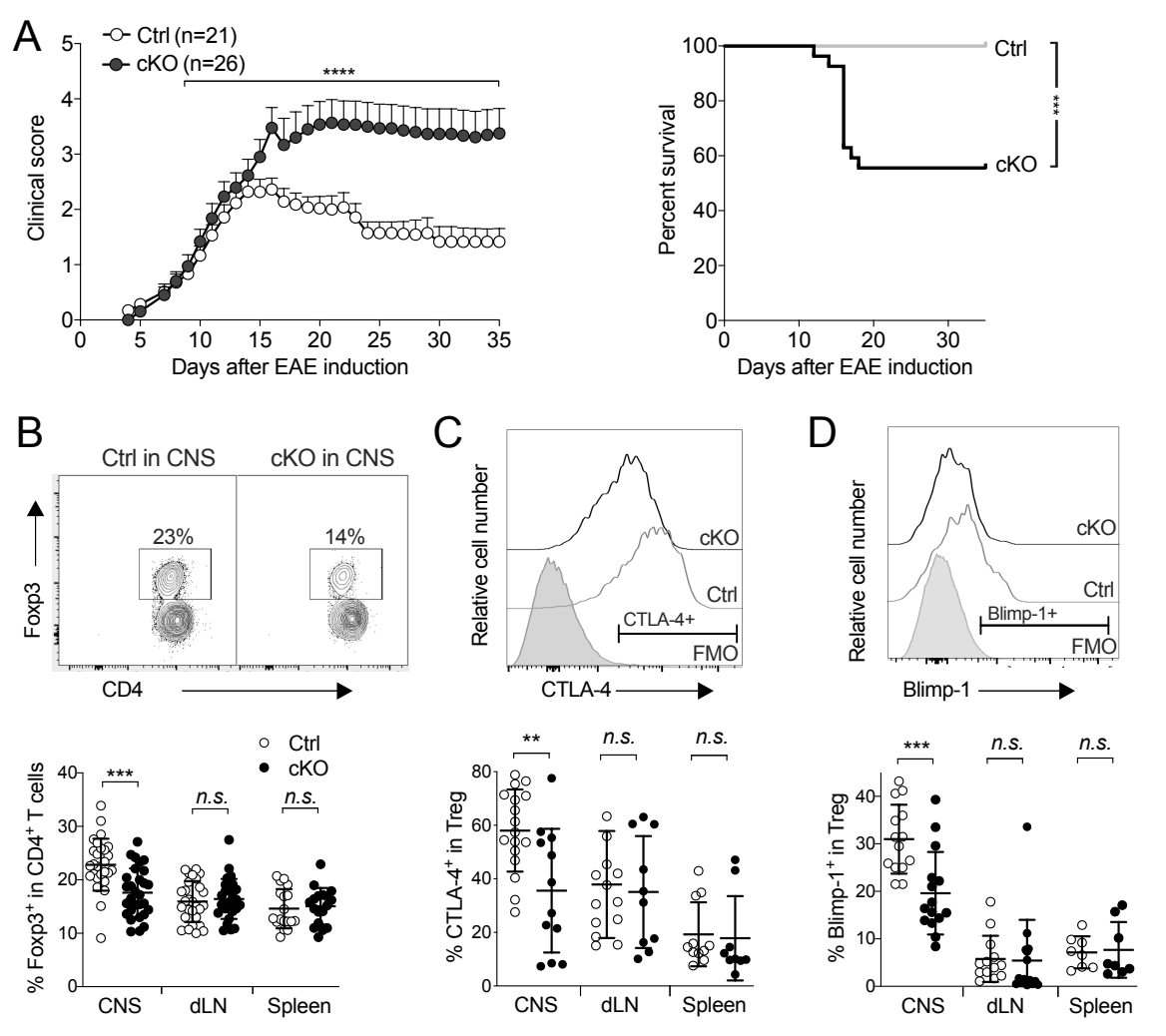
A
Ctrl (n=21)
cKO (n=26)
****
Clinical score
Days after EAE induction
Percent survival
Ctrl
cKO
***
Days after EAE induction
B
Ctrl in CNS
cKO in CNS
23%
14%
Foxp3
CD4
% Foxp3+ in CD4+ T cells
Ctrl
cKO
***
n.s.
n.s.
CNS
dLN
Spleen
C
Relative cell number
cKO
Ctrl
CTLA-4+
FMO
CTLA-4
% CTLA-4+ in Treg
**
n.s.
n.s.
CNS
dLN
Spleen
D
Relative cell number
cKO
Ctrl
Blimp-1+
FMO
Blimp-1
% Blimp-1+ in Treg
***
n.s.
n.s.
CNS
dLN
Spleen

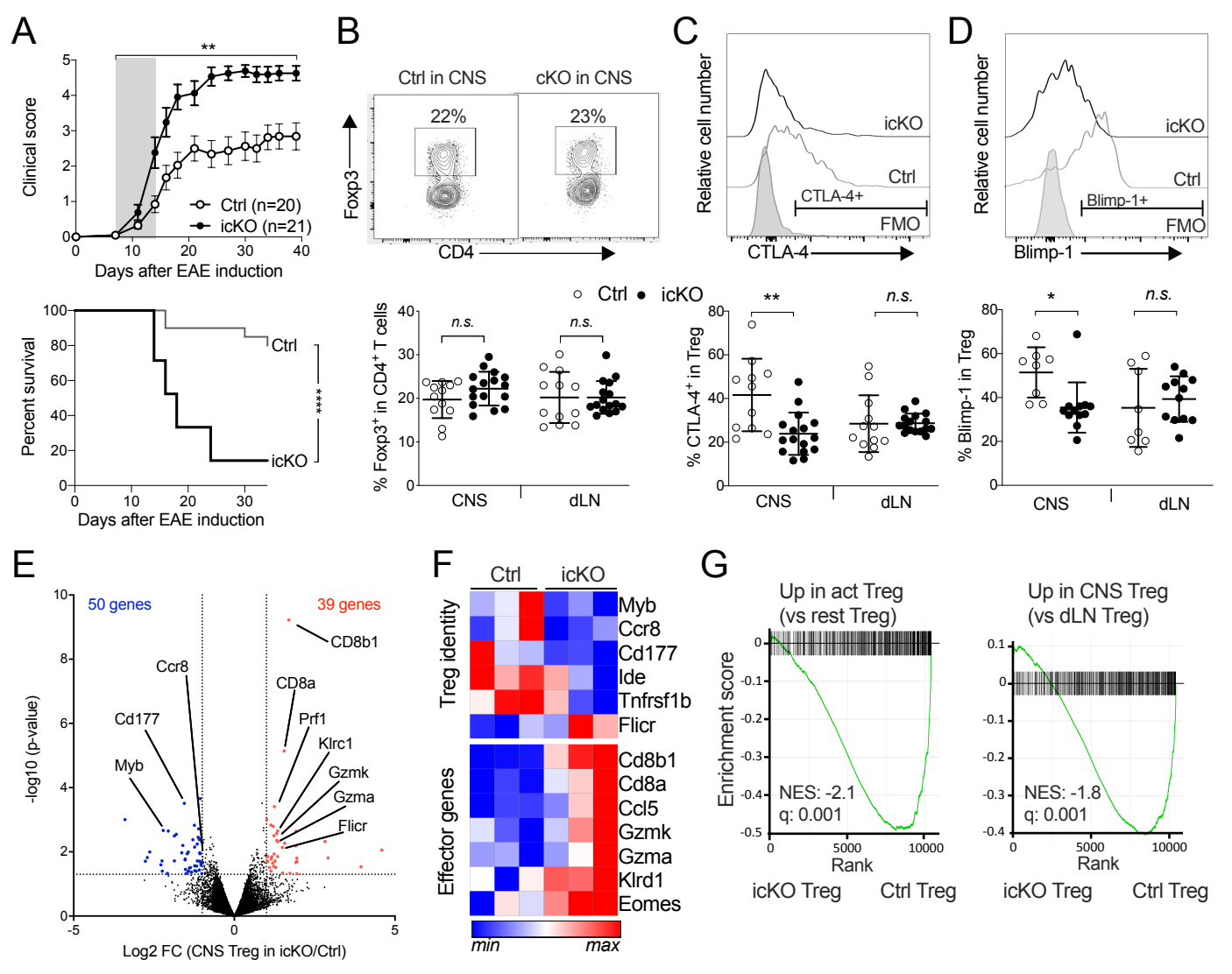
A
Clinical score
Days after EAE induction
Ctrl (n=20)
icKO (n=21)
**
B
Ctrl in CNS
cKO in CNS
22%
23%
Foxp3
CD4
C
Relative cell number
icKO
Ctrl
CTLA-4+
FMO
CTLA-4
D
Relative cell number
icKO
Ctrl
Blimp-1+
FMO
Blimp-1
Percent survival
Ctrl
icKO
****
Days after EAE induction
Ctrl
icKO
% Foxp3+ in CD4+ T cells
n.s.
n.s.
CNS
dLN
% CTLA-4+ in Treg
**
n.s.
CNS
dLN
% Blimp-1 in Treg
*
n.s.
CNS
dLN
E
50 genes
39 genes
CD8b1
Ccr8
CD8a
Cd177
Prf1
Klrc1
Myb
Gzmk
Gzma
Flicr
-log10 (p-value)
Log2 FC (CNS Treg in icKO/Ctrl)
F
Ctrl
icKO
Treg identity
Myb
Ccr8
Cd177
Ide
Tnfrsf1b
Flicr
Effector genes
Cd8b1
Cd8a
Ccl5
Gzmk
Gzma
Klrd1
Eomes
min
max
G
Up in act Treg
(vs rest Treg)
Enrichment score
NES: -2.1
q: 0.001
Rank
icKO Treg
Ctrl Treg
Up in CNS Treg
(vs dLN Treg)
NES: -1.8
q: 0.001
Rank
icKO Treg
Ctrl Treg

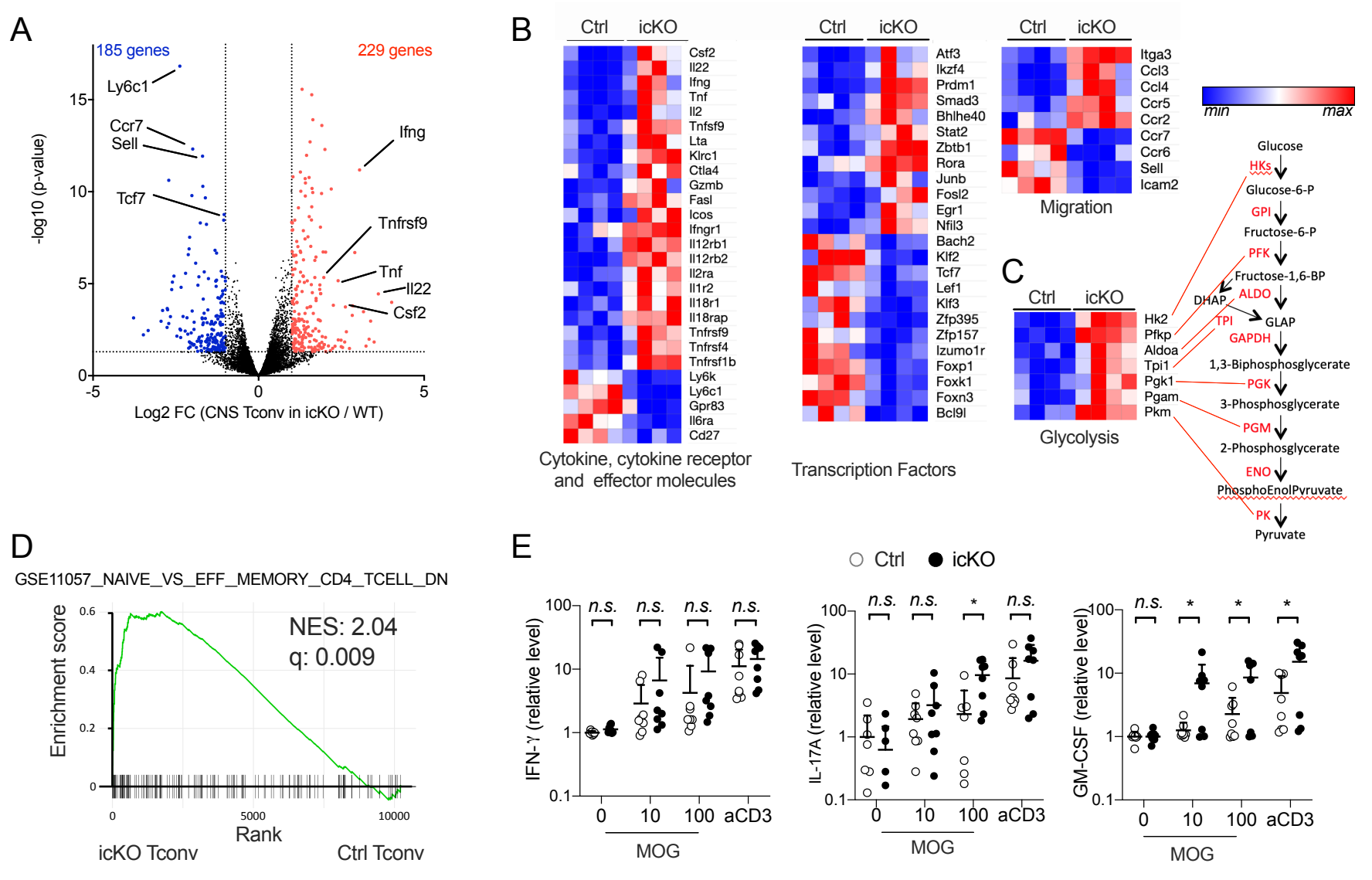
A
185 genes
229 genes
Ly6c1
Ccr7
Sell
Tcf7
Ifng
Tnfrsf9
Tnf
Il22
Csf2
-log10 (p-value)
Log2 FC (CNS Tconv in icKO / WT)
B
Ctrl
icKO
Csf2
Il22
Ifng
Tnf
Il2
Tnfsf9
Lta
Klrc1
Ctla4
Gzmb
Fasl
Icos
Ifngr1
Il12rb1
Il12rb2
Il2ra
Il1r2
Il18r1
Il18rap
Tnfrsf9
Tnfrsf4
Tnfrsf1b
Ly6k
Ly6c1
Gpr83
Il6ra
Cd27
Cytokine, cytokine receptor and effector molecules
Atf3
Ikzf4
Prdm1
Smad3
Bhlhe40
Stat2
Zbtb1
Rora
Junb
Fosl2
Egr1
Nfil3
Bach2
Klf2
Tcf7
Lef1
Klf3
Zfp395
Zfp157
Izumo1r
Foxp1
Foxk1
Foxn3
Bcl9l
Transcription Factors
Itga3
Ccl3
Ccl4
Ccr5
Ccr2
Ccr7
Ccr6
Sell
Icam2
Migration
min
max
C
Hk2
Pfkp
Aldoa
Tpi1
Pgk1
Pgam
Pkm
Glycolysis
Glucose
HKs
Glucose-6-P
GPI
Fructose-6-P
PFK
Fructose-1,6-BP
ALDO
DHAP
TPI
GLAP
GAPDH
1,3-Biphosphoglycerate
PGK
3-Phosphoglycerate
PGM
2-Phosphoglycerate
ENO
PhosphoEnolPyruvate
PK
Pyruvate
D
GSE11057_NAIVE_VS_EFF_MEMORY_CD4_TCELL_DN
NES: 2.04
q: 0.009
Enrichment score
Rank
icKO Tconv
Ctrl Tconv
E
Ctrl
icKO
IFN-γ (relative level)
IL-17A (relative level)
GM-CSF (relative level)
n.s.
*
0
10
100
aCD3
MOG

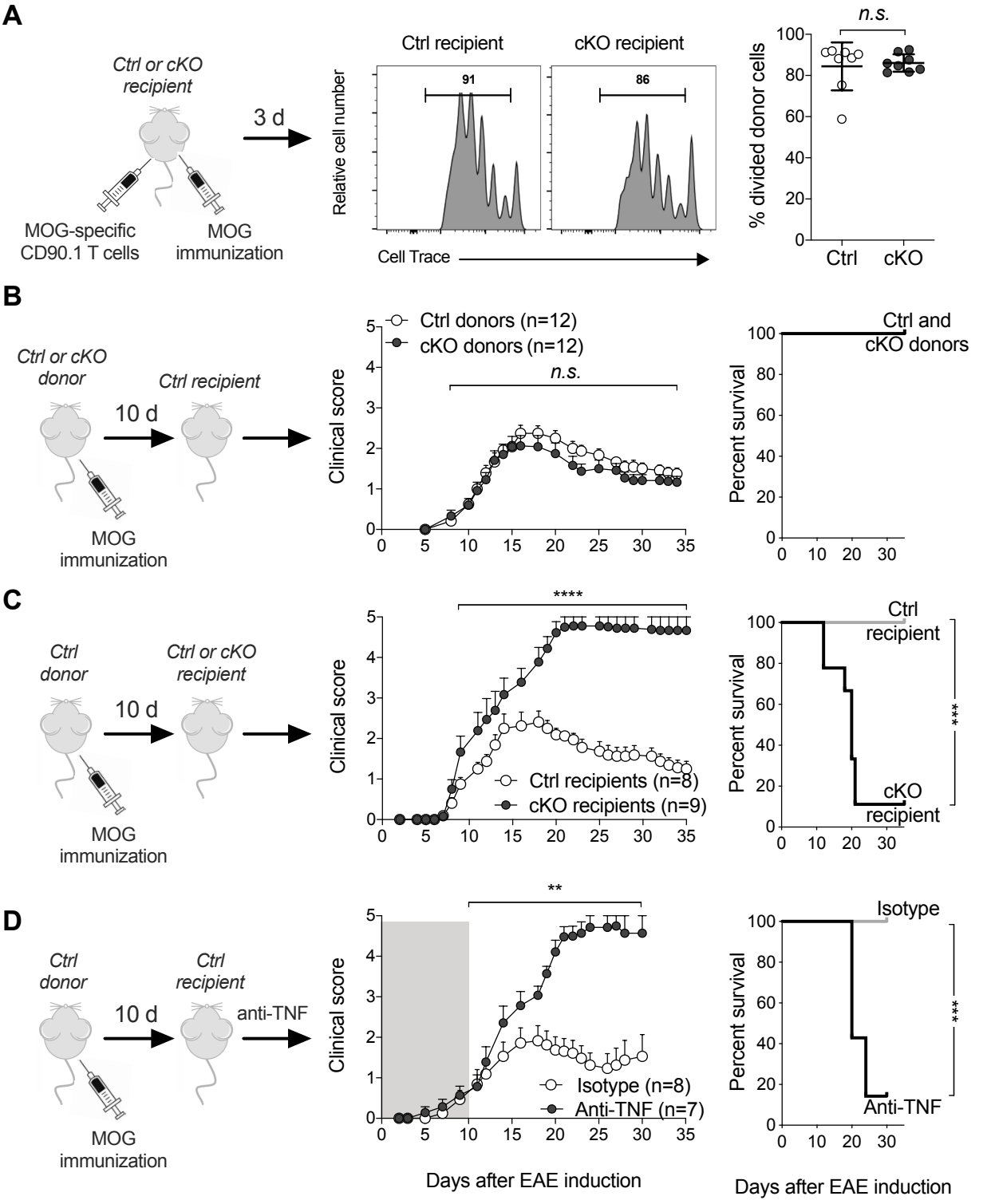
A
Ctrl or cKO recipient
3 d
MOG-specific CD90.1 T cells
MOG immunization
Ctrl recipient
cKO recipient
91
86
Relative cell number
Cell Trace
n.s.
% divided donor cells
Ctrl
cKO
B
Ctrl or cKO donor
Ctrl recipient
10 d
MOG immunization
Ctrl donors (n=12)
cKO donors (n=12)
n.s.
Clinical score
Ctrl and cKO donors
Percent survival
C
Ctrl donor
Ctrl or cKO recipient
10 d
MOG immunization
****
Ctrl recipients (n=8)
cKO recipients (n=9)
Clinical score
Ctrl recipient
cKO recipient
***
Percent survival
D
Ctrl donor
Ctrl recipient
10 d
anti-TNF
MOG immunization
**
Isotype (n=8)
Anti-TNF (n=7)
Clinical score
Days after EAE induction
Isotype
Anti-TNF
***
Percent survival
Days after EAE induction

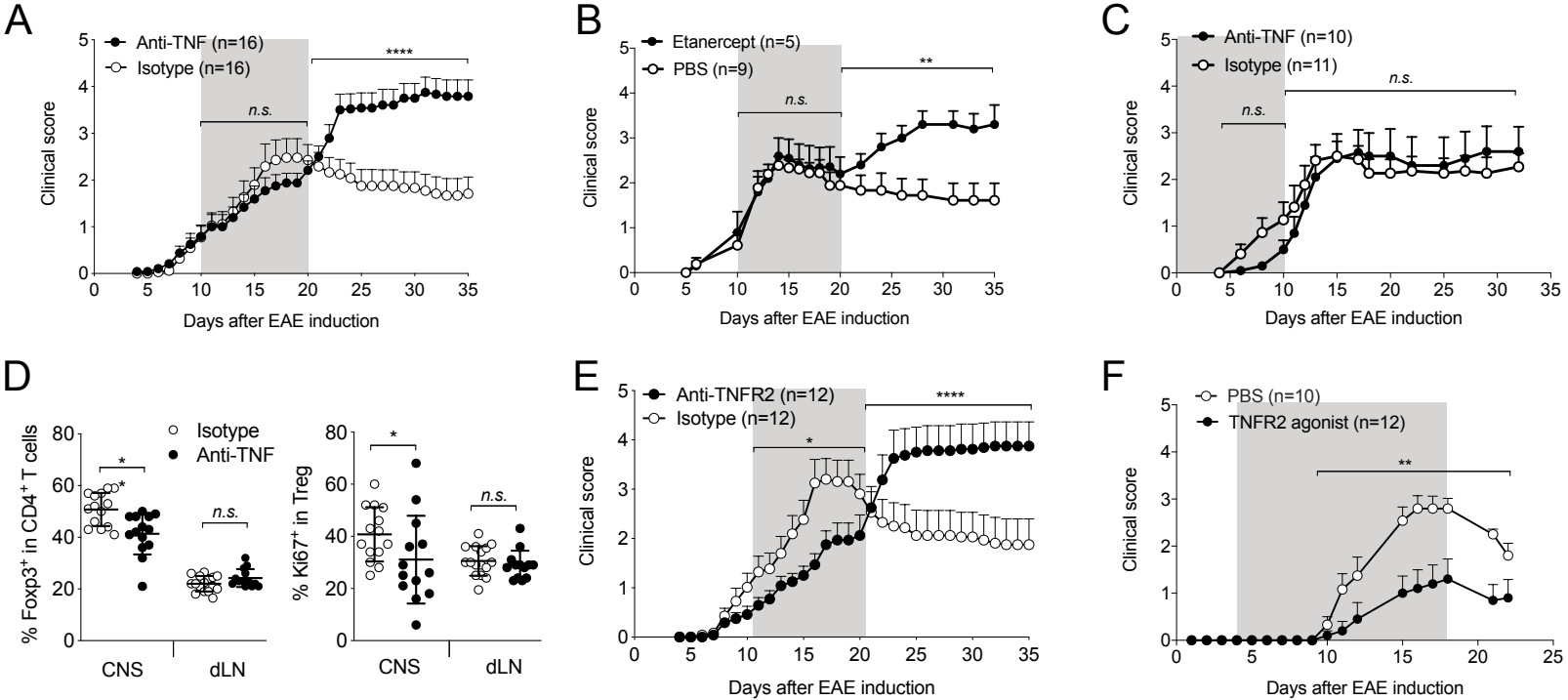
A
Anti-TNF (n=16)
Isotype (n=16)
Clinical score
Days after EAE induction
n.s.
****
B
Etanercept (n=5)
PBS (n=9)
Clinical score
Days after EAE induction
n.s.
**
C
Anti-TNF (n=10)
Isotype (n=11)
Clinical score
Days after EAE induction
n.s.
n.s.
D
Isotype
Anti-TNF
% Foxp3+ in CD4+ T cells
% Ki67+ in Treg
CNS
dLN
CNS
dLN
*
n.s.
*
n.s.
E
Anti-TNFR2 (n=12)
Isotype (n=12)
Clinical score
Days after EAE induction
*
****
F
PBS (n=10)
TNFR2 agonist (n=12)
Clinical score
Days after EAE induction
**

Supplementary Information for

Tissue-restricted control of established central nervous system autoimmunity by TNF receptor 2 expressing Treg cells

Emilie Ronin, Charlotte Pouchy, Maryam Khosravi, Morgane Hilaire, Sylvie Grégoire, Armanda Casrouge, Sahar Kassem, David Sleurs, Gaëlle H Martin, Noémie Chanson, Yannis Lombardi, Guilhem Lalle, Harald Wajant, Cédric Auffray, Bruno Lucas, Gilles Marodon, Yenkel Grinberg-Bleyer and Benoît L Salomon

Benoit Salomon. Email: benoit.salomon@inserm.fr.

Yenkel Grinberg-Bleyer. Email: yenkel.grinberg-bleyer@inserm.fr.

This PDF file includes:

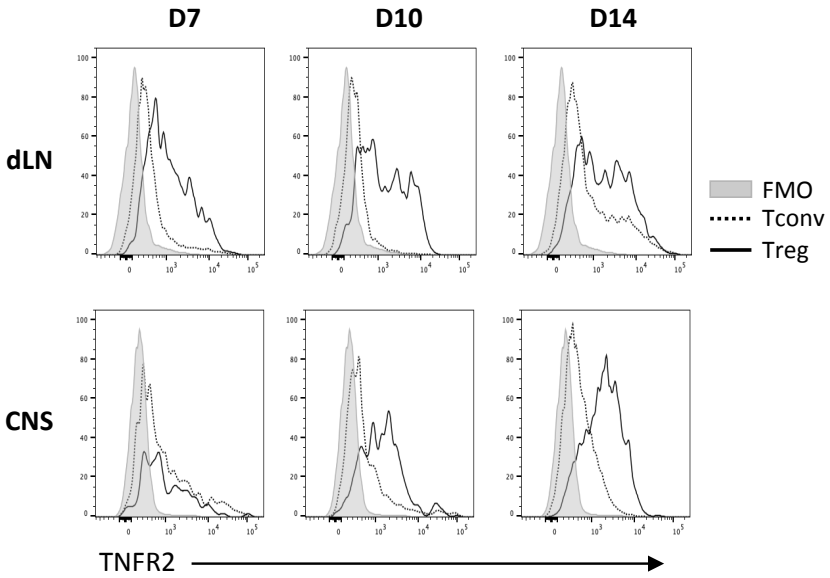

Figure S1. TNFR2 is highly expressed by Treg cells over the course of EAE. TNFR2 expression on Tconv and Treg cells, freshly isolated from dLN and CNS of C57BL/6 mice at day 7, 10 and 14 after EAE induction. Representative data from 2 independent experiments.

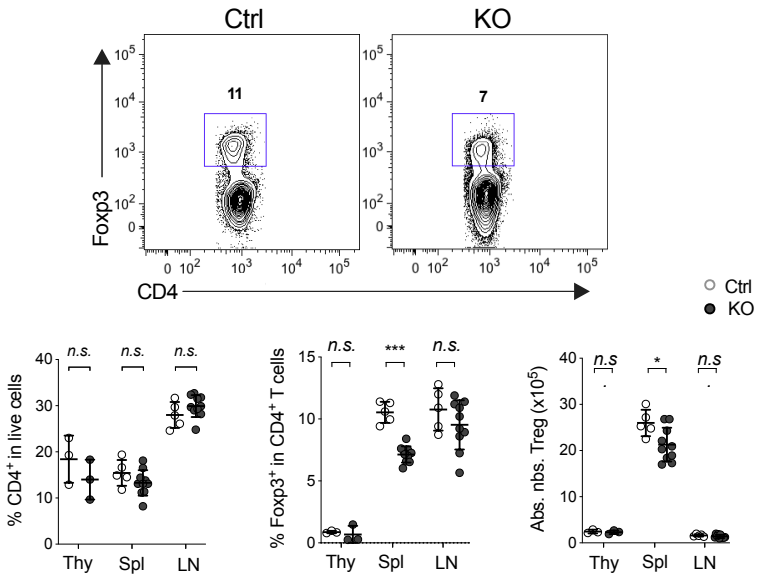

Figure S2. Partial defect of Treg cells in the spleen of Tnfrsf1b$^{-/-}$ (KO) mice. Proportions and absolute numbers of total CD4^{+} and Treg cells in KO and wild type (Ctrl) mice in the thymus (Thy), spleen (Spl) and LN. Representative flow cytometry plots in the spleen (upper panels). Each dot represents a mouse from 2 independent experiments (lower panels). Mean (+/-S.D.) is shown. Two-tailed, unpaired Mann-Whitney tests were used; ****p<0.0001, *n.s.*: not significant.

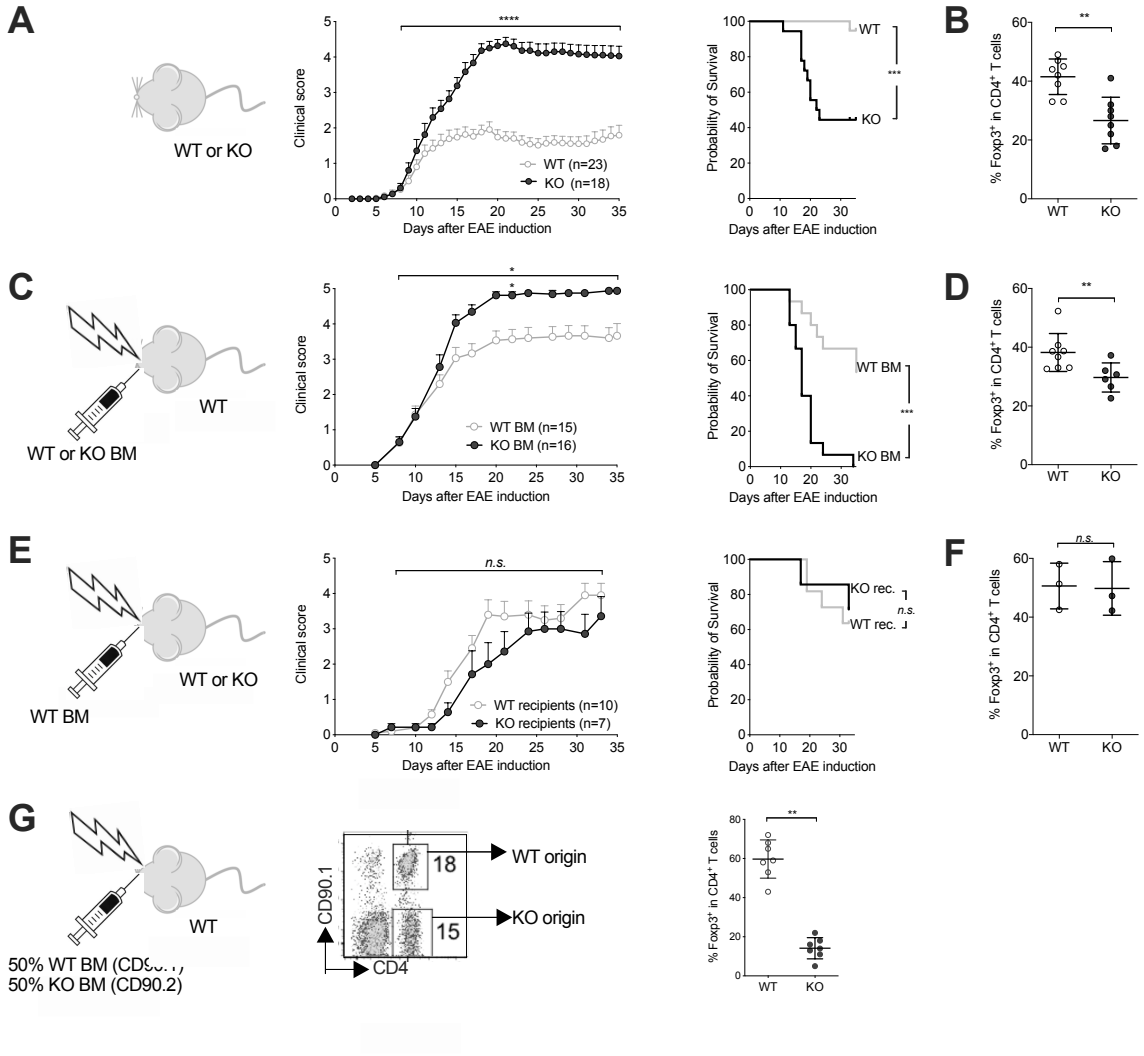

Figure S3. TNFR2 expression by hematopoietic cells is required to limit EAE severity and promotes Treg cell-intrinsic expansion in the CNS. EAE was induced in *Tnfrsf1b*$^{-/-}$ (KO) or WT littermate control mice (*A*, *B*), in WT recipients reconstituted with KO or WT bone marrow cells (*C*, *D*), in KO or WT recipients reconstituted with WT bone marrow cells (*E*, *F*), and in WT recipients reconstituted with 1:1 ratio of a mix of KO CD90.2^{+} and WT CD90.1^{+} bone marrow cells (g). EAE clinical score (Mean + SEM) and disease survival (*A*, *C*, *E*). Treg cell proportion in the CNS at day 10-15 (*B*), day 16-19 (*D*) and day 20 (*F*) and their proportion from WT or KO origins at day 20 (*G*). Data were collected from 4 (*A*, *B*) or 2 (*C*-*G*) independent experiments. Two-tailed, unpaired Mann-Whitney (for EAE scores and FACS analyses) and Log-Rank (Mantel-Cox, for survival curves) tests were used. *p<0.05, **p<0.01, ****p<0.0001, *n.s.* : not significant.

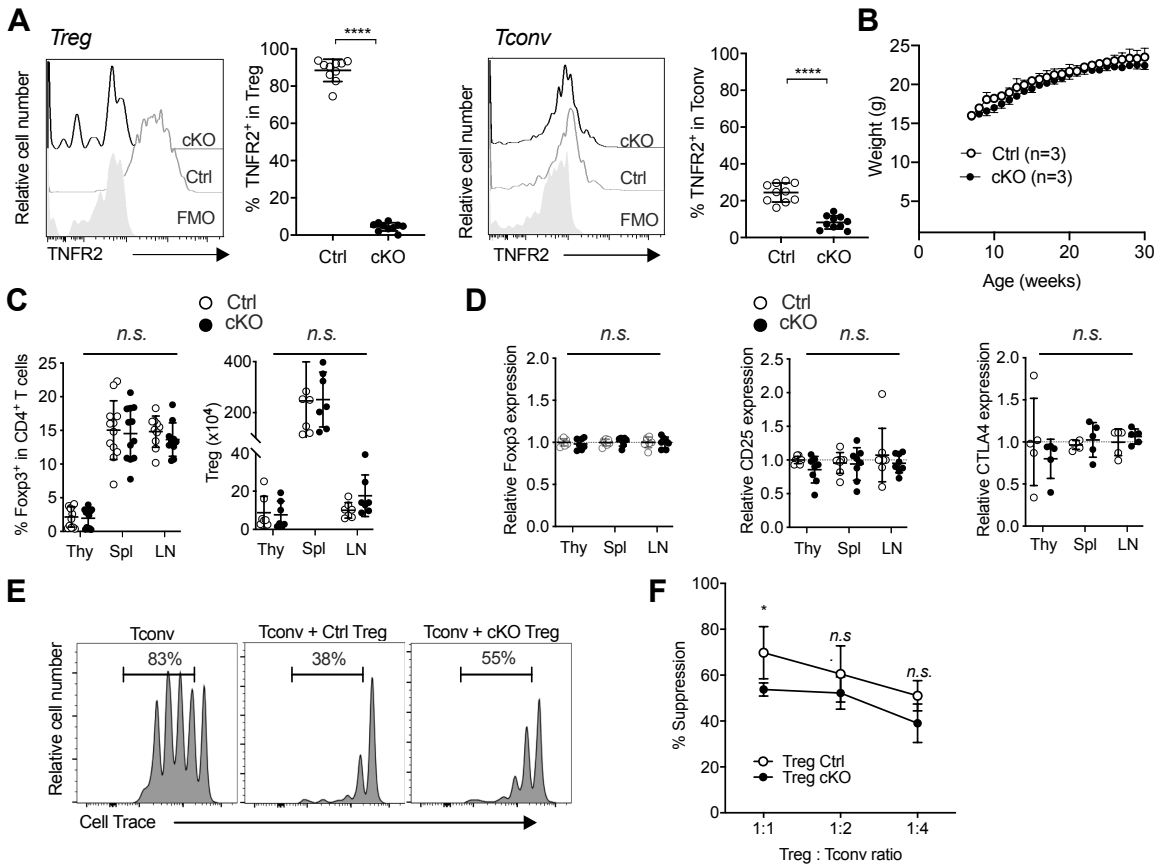

Figure S4. TNFR2 does not play a major role in Treg cell biology at steady state. (*A*) TNFR2 expression in *in vitro* activated Treg and Tconv cells, isolated from LN of *Foxp3*^{Cre}*Tnfrsf1b*$^{fl/fl}$ (cKO) and *Foxp3*^{Cre} control (Ctrl) mice. Representative data (histograms) and mean (+/- S.D.) from 3 independent experiments with each symbol representing individual mice (graphs). (*B*) Weight curves of unmanipulated females. Mean +/- S.D. is shown. (*C*) Proportion and absolute number of Treg cells in cKO and Ctrl mice in the thymus (Thy), spleen (Spl) and LN. Mean (+/- S.D) of 5 independent experiments; each dot represents a mouse. (*D*) Relative mean fluorescent intensity (MFI) of Foxp3, CD25 and CTLA-4 expression among Treg cells of cKO and Ctrl mice in the thymus, spleen and LN. The MFI of Treg cells from cKO mice divided by the average MFI of control mice is shown. Mean (+/-S.D.) is shown; each symbol represents the value of an individual mouse from 5 independent experiments. (*E*, *F) In vitro* suppressive activity of Treg cells from cKO and ctrl mice. Representative Tconv cell proliferation at the 1:2 Treg:Tconv cell ratio (*E*) and mean (+/- S.D.) at different Treg:Tconv cell ratios from 3 independent experiments (*F*). Two-tailed unpaired Mann-Whitney (a), two-way ANOVA (*C*, *D*) and paired t-tests (*F*) were used. *p<0.05, ***p<0.001, ****p<0.0001, *n.s.*: not significant.

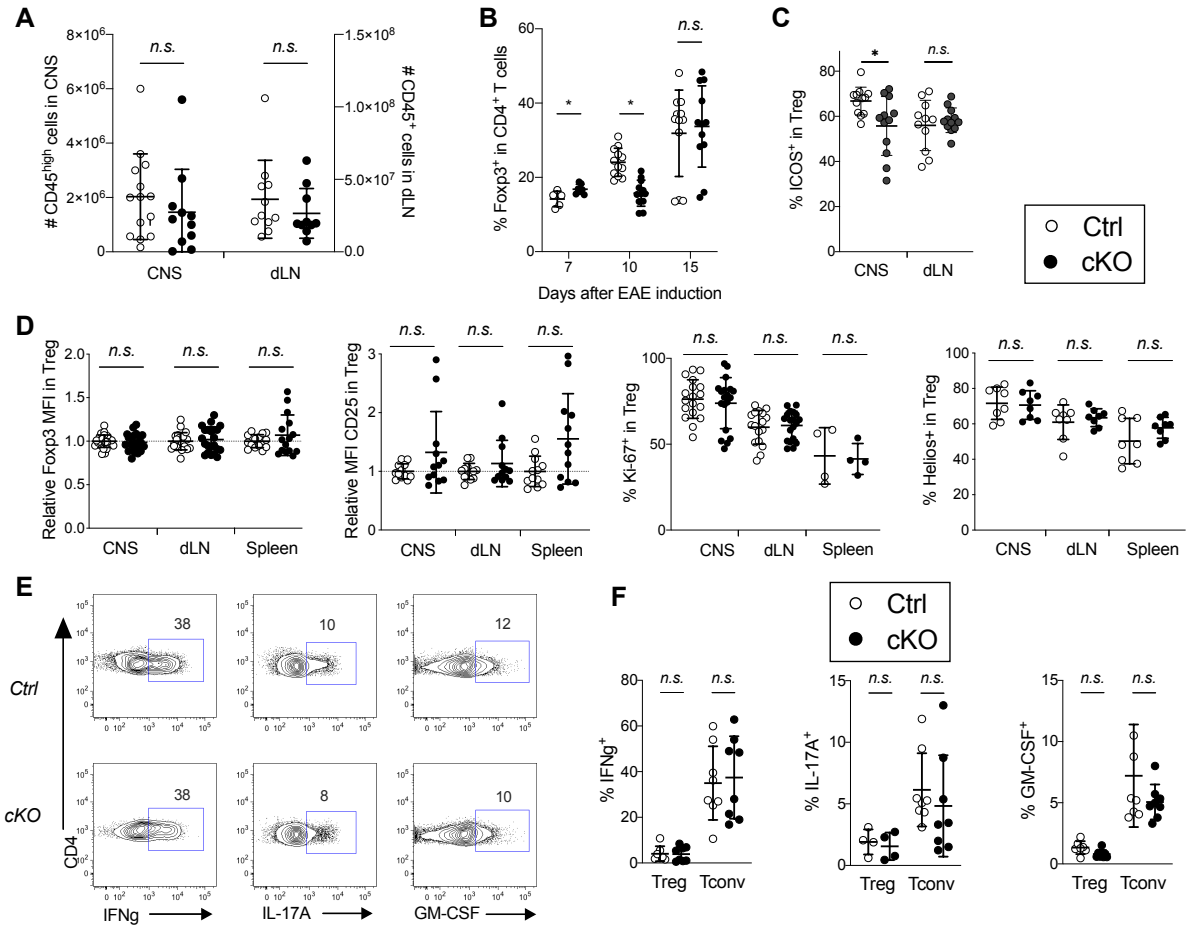

Figure S5. The decrease in Treg cell proportion in *Foxp3*^{Cre}*Tnfrsf1b*$^{f/fl}$ (cKO) mice is only transient and not associated with changes in Foxp3, Ki67, CD25 and Helios expression or cytokine production by Treg and Tconv cell subsets. EAE was induced in *Foxp3*^{Cre}*Tnfr2*$^{fl/fl}$ (cKO) and *Foxp3*^{Cre} control (Ctrl) mice. (*A*) Absolute numbers of CD45^{high} and CD45^{+} cells in the CNS and dLN at day 10. (*B*) Treg cell proportion in the CNS of cKO and Ctrl mice at day 7, 10 and 15. Proportion of ICOS^{+} (*C*), Ki67^{+} and Helios^{+} among Treg cells and relative MFI of Foxp3 and CD25 among Treg cells (D), calculated as in Fig. S4*D*, at day 10. Representative flow cytometry plots in Tconv cells (*E*) and proportions in Treg or Tconv cells (*F*) of IFNγ^{+}, IL-17A^{+} and GM-CSF^{+} cells after PMA-ionomycine stimulation in the CNS of Ctrl and cKO mice at day 10. Mean (+/-S.D.) is shown. Each symbol represents the value of an individual mouse from 4 (*A*), 2 (*B*, day 7), 4 (*B*, day 10), 5 (*B*, day 15), 5 (*C*) and 2 to 5 (*D, F*) independent experiments. Two-tailed, unpaired Mann-Whitney tests were used; *p<0.05, *n.s.*: not significant.

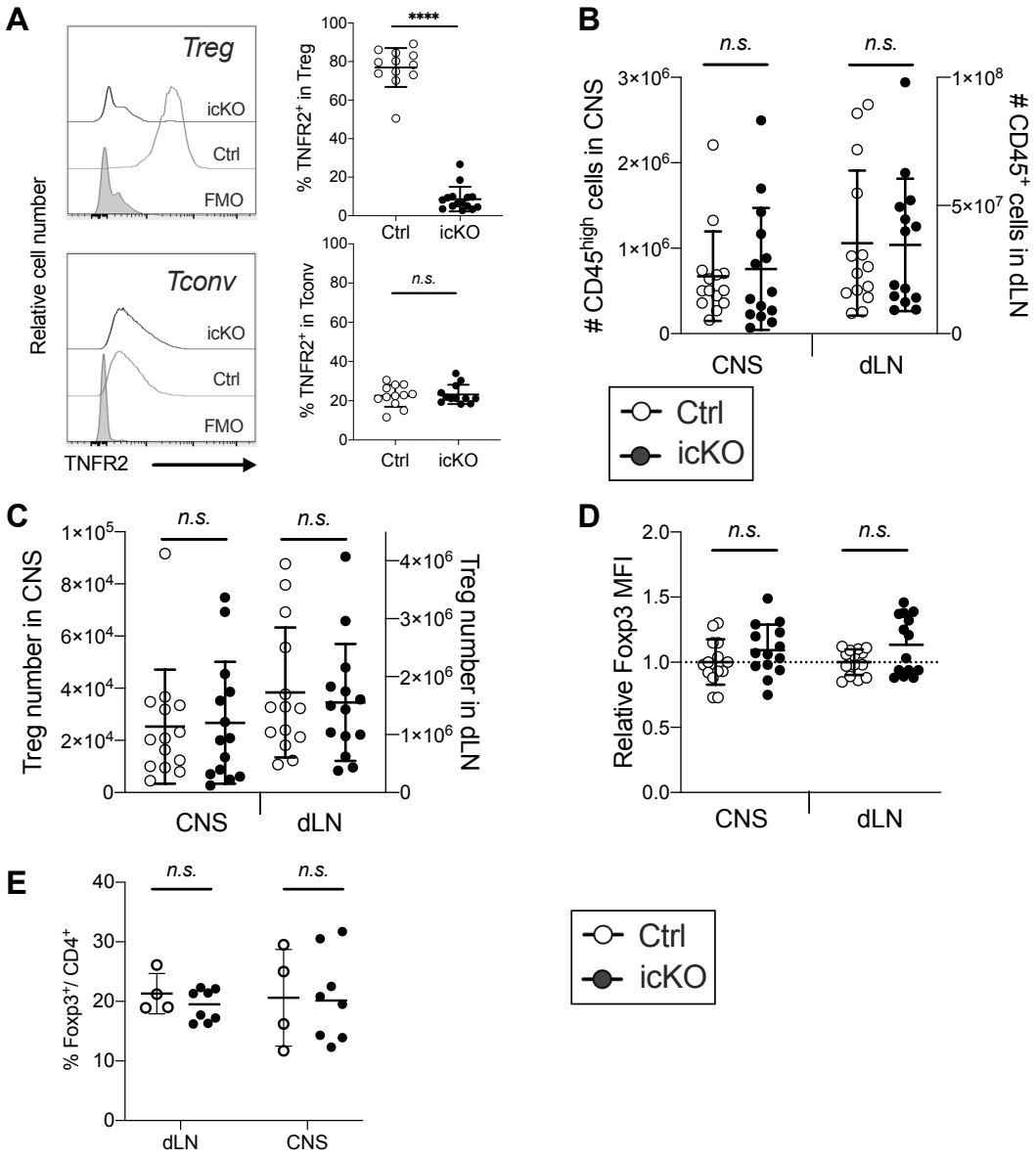

Figure S6. TNFR2 deletion in *Foxp3*$^{Cre\text{-}ERT2}$*Tnfrsf1b*^{fl} (icKO) mice is Treg specific and does not impact on their number or Foxp3 expression during EAE. *Foxp3*$^{Cre\text{-}ERT2}$*Tnfrsf1b*^{fl} (icKO) and *Foxp3*$^{Cre\text{-}ERT2}$ (Ctrl) mice were immunized to induce EAE at day 0, treated with tamoxifen from day 7 to 14 and analyzed at day 14 (*A-D*) or day 10 (*E*). (*A*) TNFR2 expression in *in vitro* activated Treg and Tconv cells, isolated from LN. Representative data (left panels) and mean (+/- S.D.) from 3 independent experiments with each symbol representing individual mice (right panels). Number of leukocytes (*B*), Treg cells (*C*) and Foxp3 expression level in Treg cells calculated as in Fig. S4*D* (*D*) in the CNS and dLN. (*E*) Treg cell proportion in dLN and CNS at day 10. Means (+/- S.D.) were obtained from 5 (*B-D*) or 2 (*E*) independent experiments. Two-tailed, unpaired Mann-Whitney tests were used *; n.s.*: not significant, ****p<0.0001

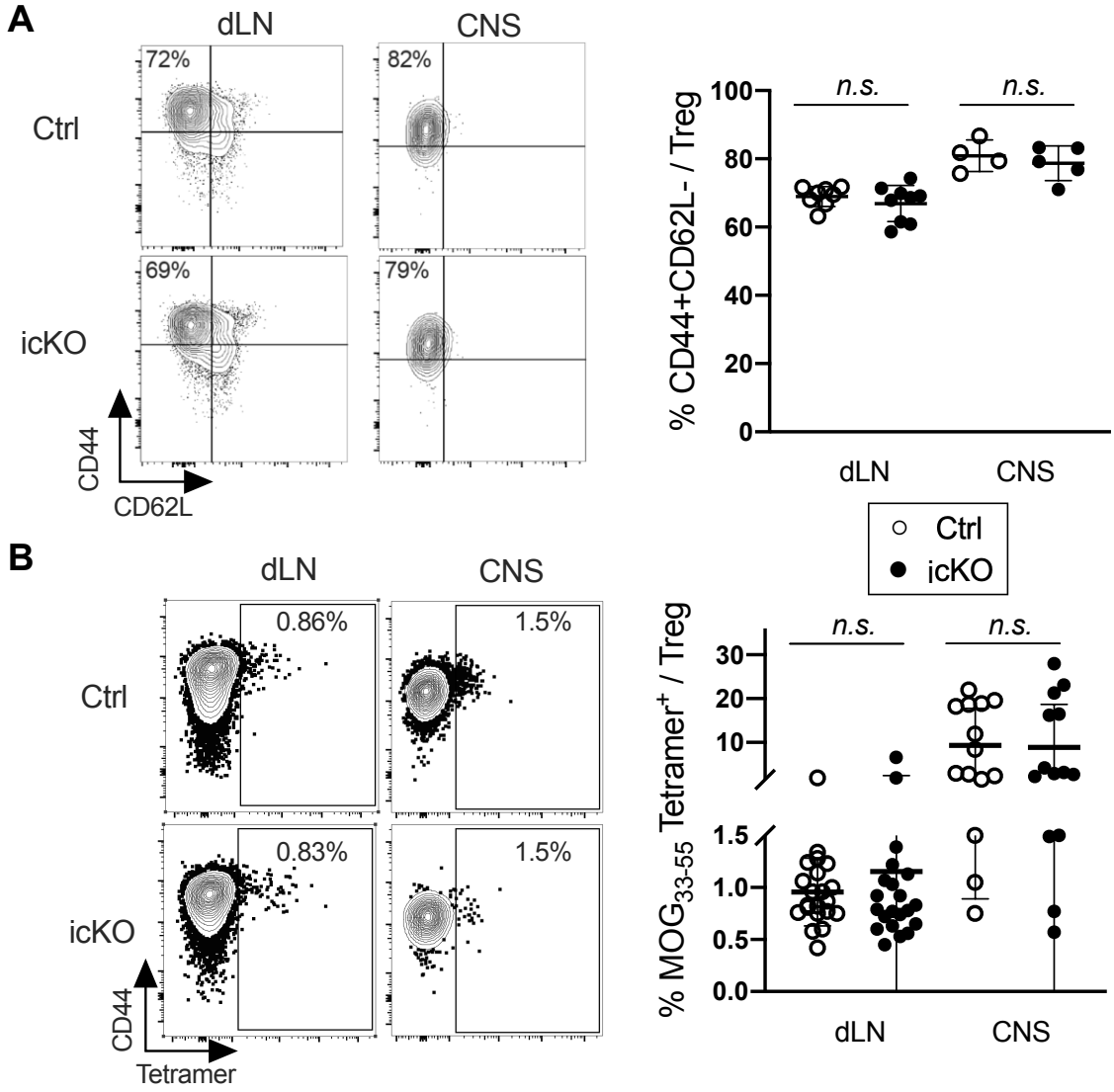

Figure S7. Similar proportions of activated and MOG-specific Treg cells in *Foxp3*$^{Cre\text{-}ERT2}$*Tnfrsf1b*^{fl} (icKO) and control mice. *Foxp3*$^{Cre\text{-}ERT2}$*Tnfrsf1b*^{fl} (icKO) and *Foxp3*$^{Cre\text{-}ERT2}$ (Ctrl) mice were immunized to induce EAE at day 0, treated with tamoxifen from day 7 to 14 and analyzed at day 14. Representative flow cytometry plots (left panels) and proportions (right panels) of CD44^{+}CD62L^{-} (*A*) and MOG$_{35\text{-}55}$-specific (Tetramer^{+}) (*B*) cells among Treg cells in the dLN and CNS. Mean (+/-S.D.) is shown. Each symbol represents the value of an individual mouse from 2 or 3 independent experiments. Two-tailed, unpaired Mann-Whitney tests were used; *n.s.*: not significant.

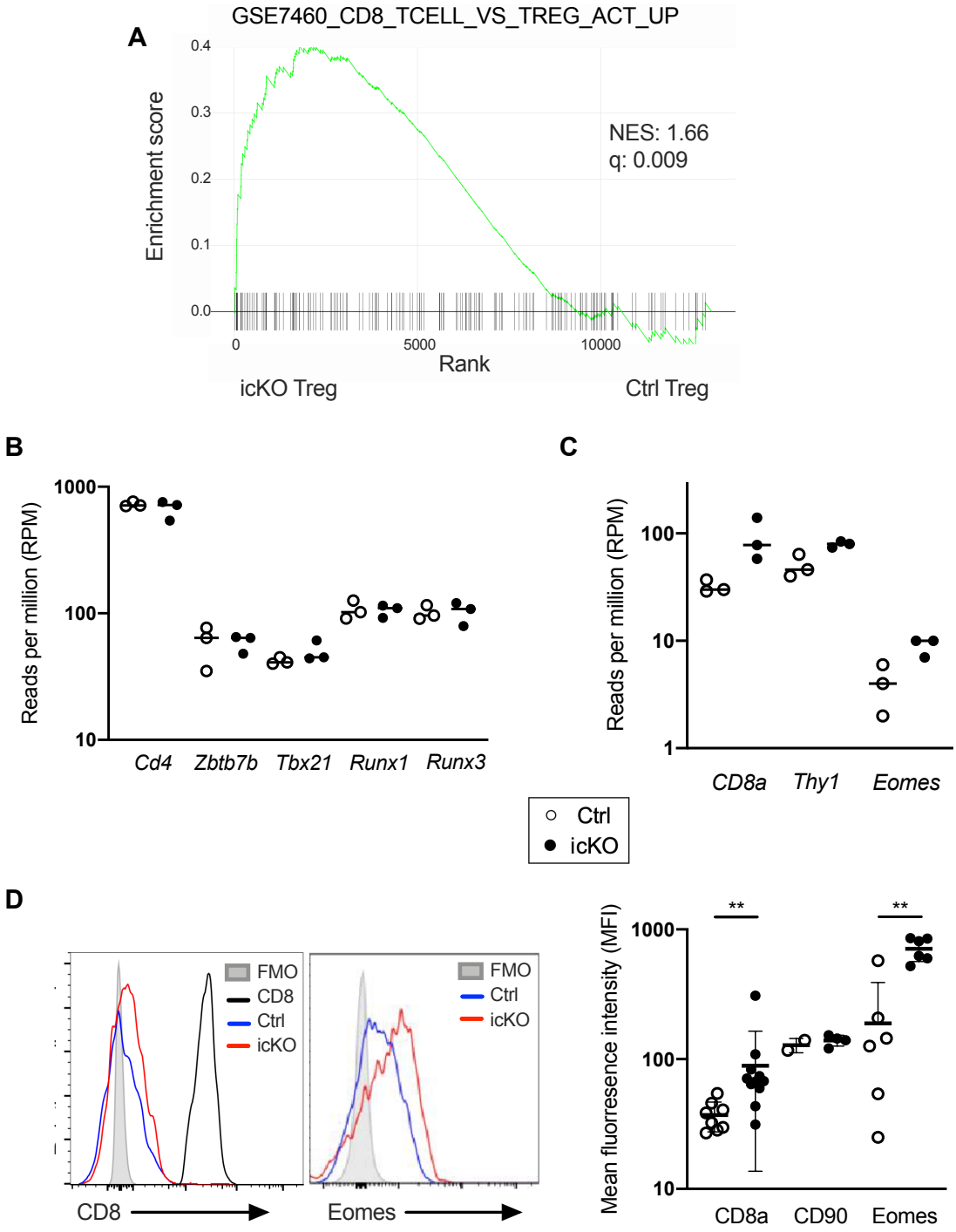

Figure S8. Validation of RNA expression at the protein level in CNS Treg cells. *Foxp3*$^{Cre\text{-}ERT2}$*Tnfrsf1b*^{fl} (icKO) and *Foxp3*$^{Cre\text{-}ERT2}$ (Ctrl) mice were immunized to induce EAE at day 0, treated with tamoxifen from day 7 to 14, and CNS Treg cells were analyzed at day 14. (*A*) GSEA analysis showing an enrichment of the CD8 Tconv cell signature by TNFR2-deficient compared to Ctrl Treg cells. (*B*, *C*) Expression levels of *Cd4*, *Zbtb7b*, *Tbx21*, *Runx1*, *Runx3* (*B*) and *CD8a*, *Thy1*, *Eomes* (*C*) genes, as determined from RNA-seq data. (*D*) Representative histograms (left panels) and mean (+/-S.D., right panel) of expression level of CD8a, CD90 (encoded by *Thy1*) and Eomes proteins analyzed by flow cytometry. Each symbol represents the value of an individual mouse from 2 to 3 independent experiments. Two-tailed, unpaired Mann-Whitney tests were used; **p<0.01.

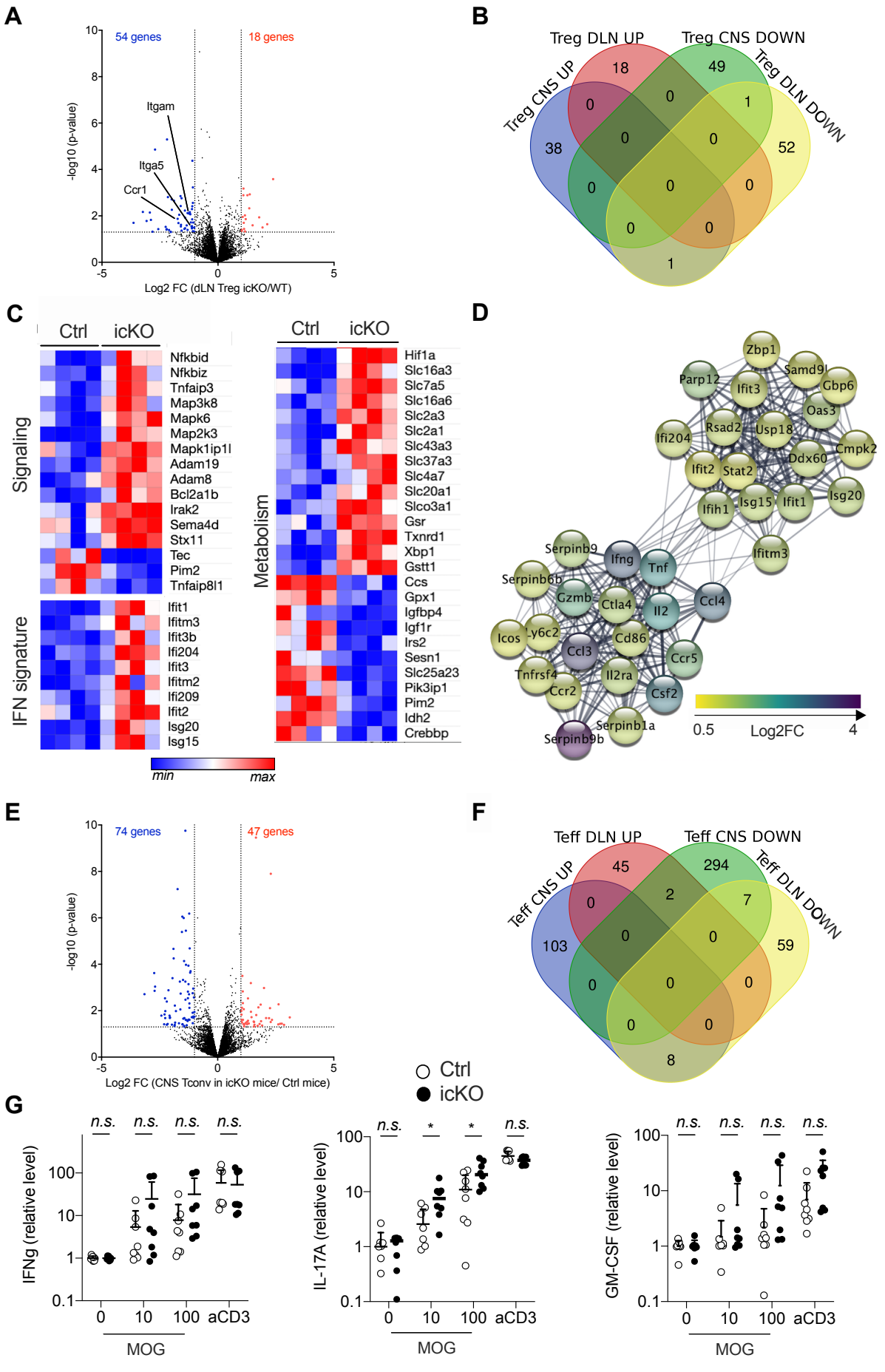
A
54 genes
18 genes
Itgam
Itga5
Ccr1
-log10 (p-value)
Log2 FC (dLN Treg icKO/WT)
B
Treg DLN UP
Treg CNS DOWN
Treg CNS UP
Treg DLN DOWN
18
49
38
52
1
1
C
Ctrl
icKO
Signaling
IFN signature
Metabolism
Nfkbid
Nfkbiz
Tnfaip3
Map3k8
Mapk6
Map2k3
Mapk1ip1l
Adam19
Adam8
Bcl2a1b
Irak2
Sema4d
Stx11
Tec
Pim2
Tnfaip8l1
Ifit1
Ifitm3
Ifit3b
Ifi204
Ifit3
Ifitm2
Ifi209
Ifit2
Isg20
Isg15
Hif1a
Slc16a3
Slc7a5
Slc16a6
Slc2a3
Slc2a1
Slc43a3
Slc37a3
Slc4a7
Slc20a1
Slco3a1
Gsr
Txnrd1
Xbp1
Gstt1
Ccs
Gpx1
Igfbp4
Igf1r
Irs2
Sesn1
Slc25a23
Pik3ip1
Pim2
Idh2
Crebbp
min
max
D
Zbp1
Samd9l
Parp12
Ifit3
Gbp6
Oas3
Rsad2
Usp18
Ifi204
Cmpk2
Ddx60
Ifit2
Stat2
Isg20
Ifih1
Isg15
Ifit1
Ifitm3
Serpinb9
Ifng
Tnf
Serpinb6b
Gzmb
Ctla4
Il2
Ccl4
Icos
Cd86
Ccl3
Ccr5
Tnfrsf4
Il2ra
Ccr2
Csf2
Serpinb1a
Serpinb9b
0.5
Log2FC
4
E
74 genes
47 genes
-log10 (p-value)
Log2 FC (CNS Tconv in icKO mice/ Ctrl mice)
F
Teff DLN UP
Teff CNS DOWN
Teff CNS UP
Teff DLN DOWN
45
294
103
59
8
G
Ctrl
icKO
IFNg (relative level)
IL-17A (relative level)
GM-CSF (relative level)
n.s.
*
0
10
100
aCD3
MOG

Figure S9. Gene expression and cytokine production by dLN- and CNS- derived Treg cells and Tconv cells. EAE was induced in *Foxp3*$^{Cre\text{-}ERT2}$*Tnfrsf1b*^{fl} (icKO) and *Foxp3*$^{Cre\text{-}ERT2}$ (Ctrl) mice, treated with tamoxifen as in Fig. 5 and analyzed at day 14. Volcano plot of DEG in DLN-Treg cells (*A*) and DLN-Tconv cells (*E*). Venn diagrams showing the comparison of DEG (Log2FC<-1 or >1, p<0.05) between CNS and dLN isolated Treg cells (B) and Tconv cells (F) using <http://bioinformatics.psb.ugent.be/webtools/Venn/> and Cytoscape v3.7. (*C*) Heatmaps showing expression of selected genes (FDR<0.05) belonging to the signaling, IFN signature and metabolic (excluding enzymes of the glycolysis) pathways, in CNS-Tconv cells. (*D*) Network analysis of putative protein-protein interaction of genes up-regulated (FDR<0.05 Log2FC>0.5) in CNS-Tconv cells of icKO mice relative to controls using the STRING application in Cytoscape v3.7 (1, 2). (*G*) Cytokines produced by dLN cells re-stimulated ex-vivo by the immunizing MOG antigen or an anti-CD3 mAb were measured in the supernatants by ELISA. Graphs show the fold change concentration over control un-stimulated cells. Pool of 2 independent experiments with each symbol representing an individual mouse. 2-way unpaired ANOVA test with Sidak correction for multiple comparisons. *p<0.05, *n.s. : not* significant.

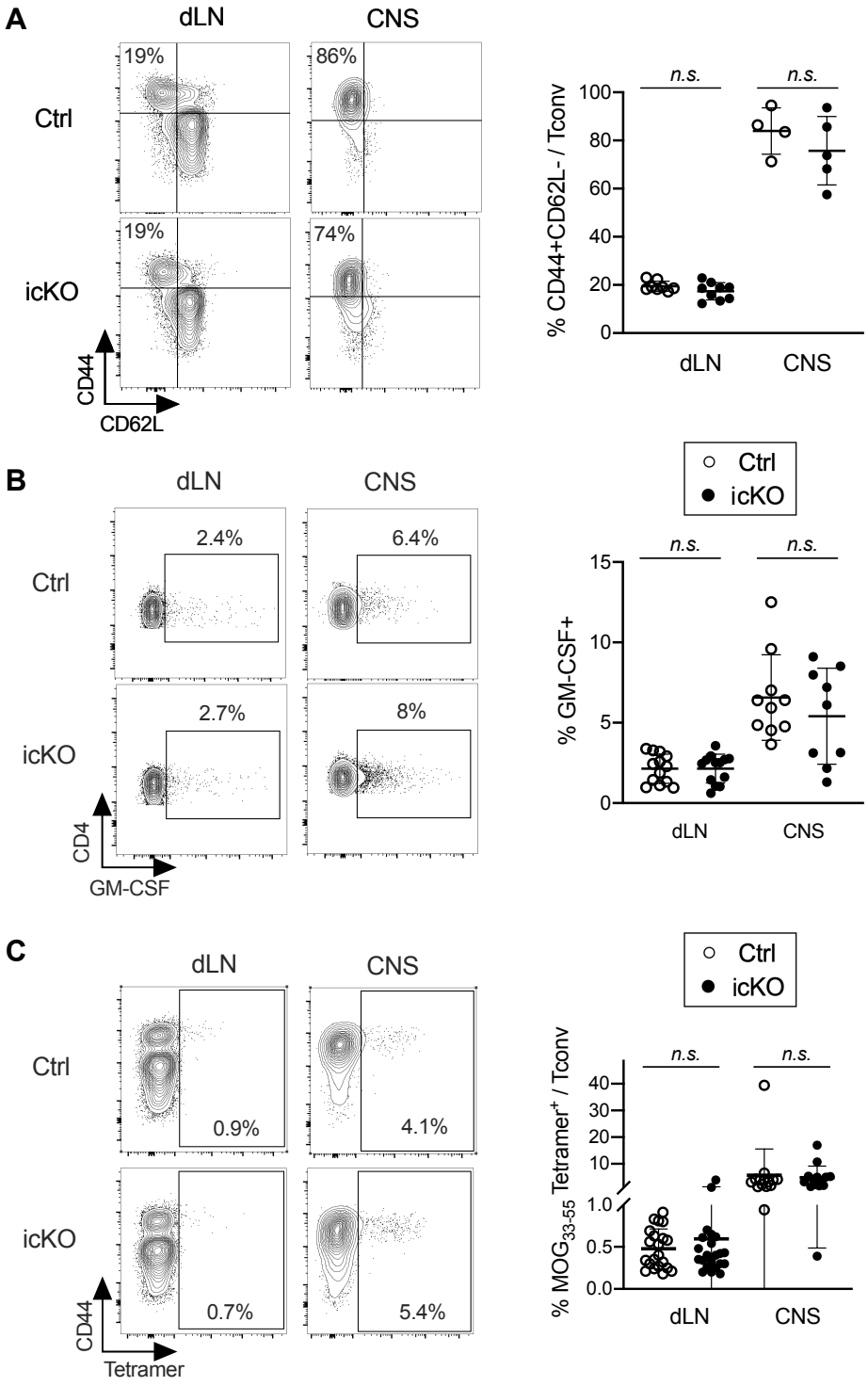

Figure S10. Similar activation and specificity of Tconv cells in *Foxp3*$^{Cre\text{-}ERT2}$*Tnfrsf1b*^{fl} (icKO) and control mice. *Foxp3*$^{Cre\text{-}ERT2}$*Tnfrsf1b*^{fl} (icKO) and *Foxp3*$^{Cre\text{-}ERT2}$ (Ctrl) mice were immunized to induce EAE at day 0, treated with tamoxifen from day 7 to 14 and analyzed at day 14. Representative flow cytometry plots (left panels) and proportion (right panels) of CD44^{+}CD62L^{-} (*A*), GM-CSF^{+} (*B*) and MOG-specific cells (Tetramer) (*C*) cells among Treg cells in the dLN and CNS. For cytokine detection, cells were stimulated by PMA-ionomycine. Mean (+/-S.D.) is shown. Each symbol represents the value of an individual mouse from 2 or 3 independent experiments. Two-tailed, unpaired Mann-Whitney tests were used; *n.s.*: not significant.

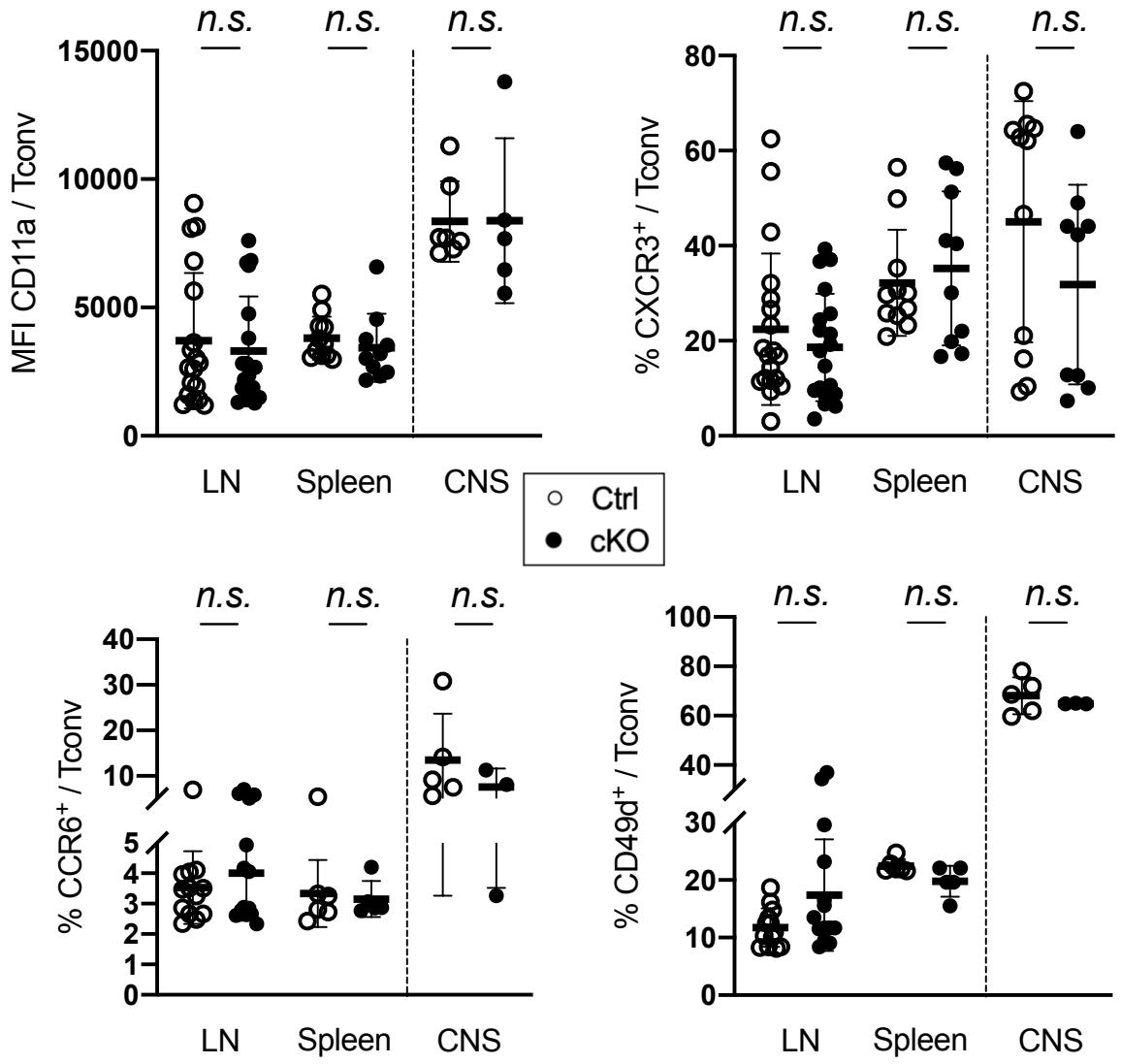

Figure S11. Tconv cells of *Foxp3^{Cre}Tnfrsf1b^{fl}* (cKO) mice exhibit normal expression of molecules involved in migration to the inflamed CNS. *Foxp3^{Cre}Tnfrsf1b^{fl}* (cKO) and *Foxp3^{Cre}* control (Ctrl) were immunized to induce EAE at day 0 and analyzed at day 10. Expression level of CD11a and proportions of CXCR3^{+}, CCR6^{+} and CD49d^{+} cells among Tconv cells in the LN, spleen and CNS analyzed by flow cytometry. Mean (+/-S.D.) is shown. Each symbol represents the value of an individual mouse from 3 independent experiments. Two-tailed, unpaired Mann-Whitney tests were used; *n.s.*: not significant.

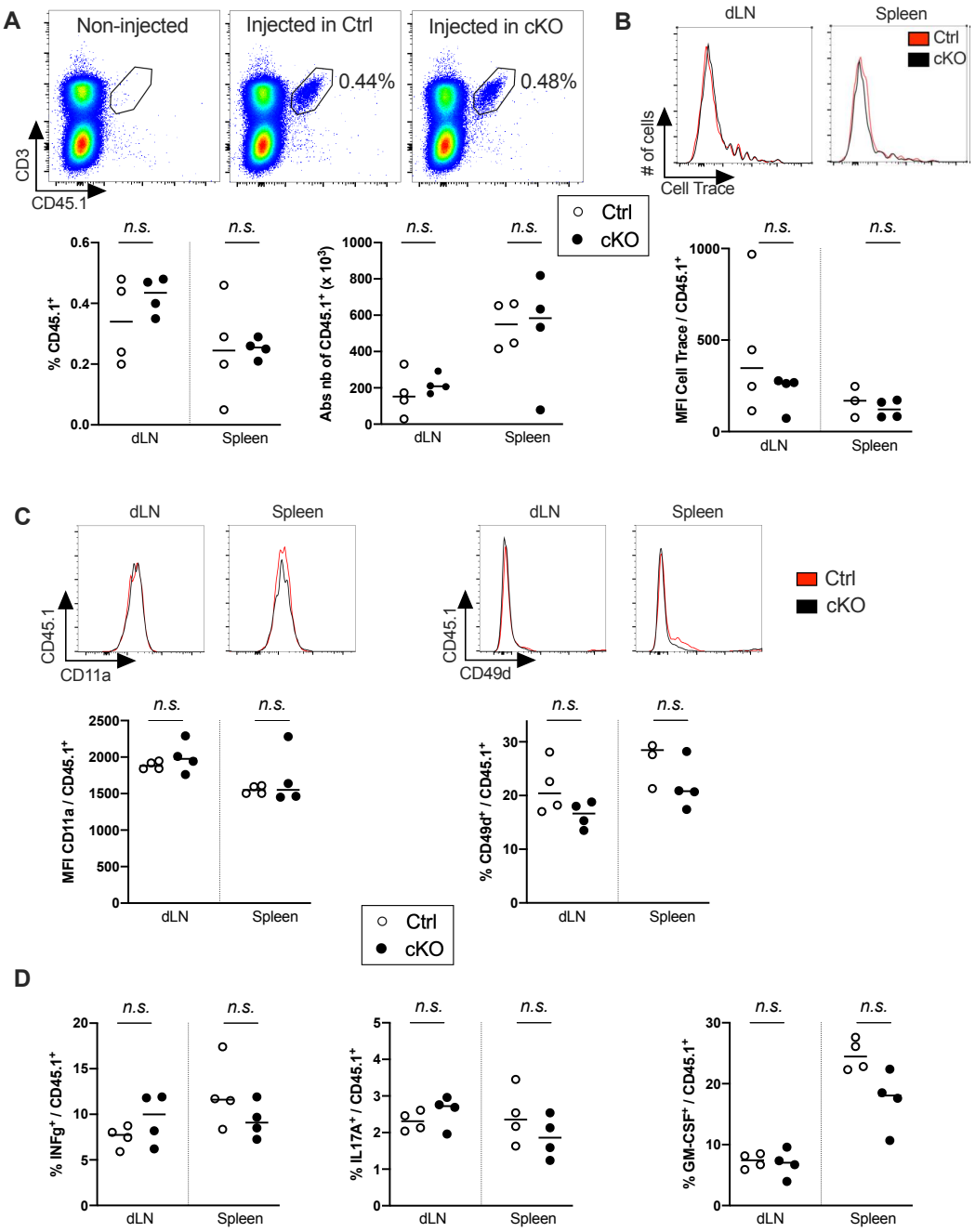

Figure S12. MOG-specific Tconv cells are primed similarly in *Foxp3*^{Cre}*Tnfrsf1b*$^{fl/fl}$ (cKO) and *Foxp3*^{Cre} control (Ctrl). MOG-specific Tconv cells collected from 2D2 CD45.1 mice were adoptively transferred in *Foxp3*^{Cre}*Tnfrsf1b*$^{fl/fl}$ (cKO) and *Foxp3*^{Cre} control (Ctrl) mice, which were immunized for EAE induction the day after and analyzed 7 days later in the dLN and spleen. (*A*) Representative flow cytometry plots (dLN, top panels) and proportions and numbers (bottom panel) of MOG-specific donor Tconv cells (CD3^{+}CD45.1^{+}). (*B*) Representative data (histograms) and MFI of cell trace dilution in injected MOG-specific donor Tconv cells. (*C*) Representative data (histograms), expression lever of CD11a and proportion of CD49d^{+} cells in injected MOG-specific donor Tconv cells. (*D*) Proportions of IFNg^{+}, IL-17A^{+} and GM-CSF^{+} in injected MOG-specific donor Tconv cells after PMA-ionomycine stimulation. Mean (+/-S.D.) is shown. Each symbol represents the value of an individual mouse from 2 independent experiments. Two-tailed, unpaired Mann-Whitney tests were used; *n.s.*: not significant.

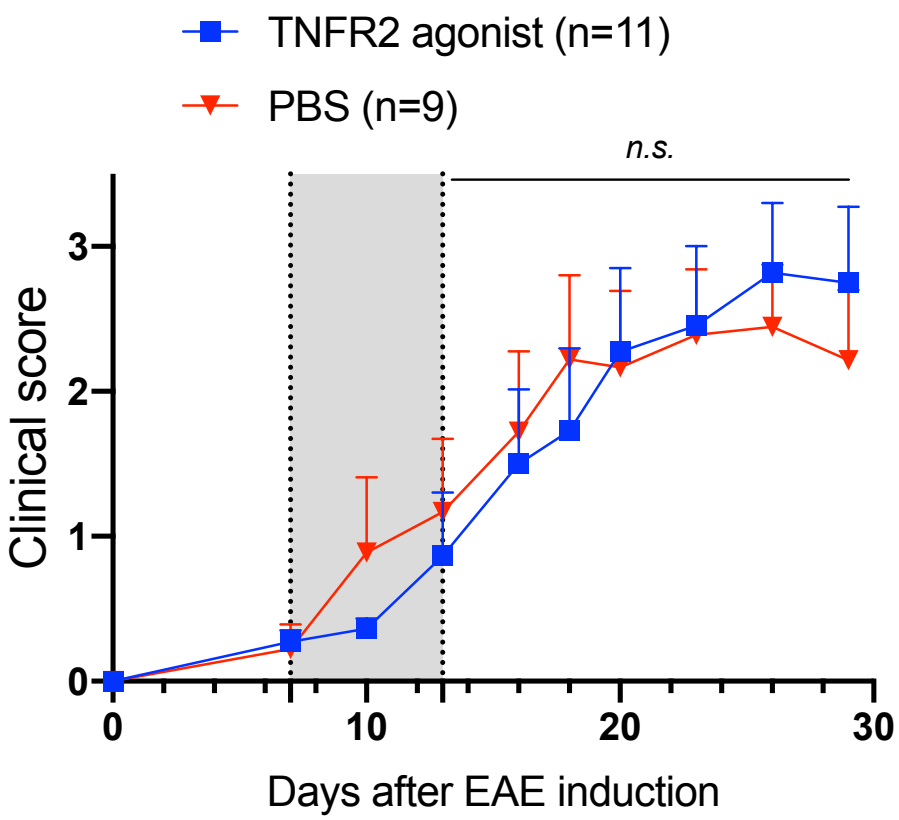

Figure S13. Therapeutic effect of a TNFR2 agonist is dependent on TNFR2 expression by Treg cells. EAE clinical score of *Foxp3*$^{Cre\text{-}ERT2}$*Tnfrsf1b*^{fl} (icKO) mice that were immunized to induce EAE at day 0, treated with tamoxifen from day 7 to 14, and with PBS or a TNFR2 agonist from day 4 to 18. Mean (+ SEM) from 2 independent experiments is shown. Two-tailed unpaired Mann-Whitney test was used. *n.s.*: not significant.

SI References (for Figure S9)

1. Doncheva, N.T., Morris, J.H., Gorodkin, J., and Jensen, L.J. Cytoscape StringApp: Network Analysis and Visualization of Proteomics Data. *J Proteome Res*. 18, 623-632 (2019).
2. Shannon, P., et al. Cytoscape: a software environment for integrated models of biomolecular interaction networks. *Genome Res*.13, 2498-2504 (2003).